

CAPILLARY ELECTROPHORESIS–MASS SPECTROMETRY
SEPARATION OF ISOMERIC BIOLOGICAL COMPOUNDS

by

Laiel Soliman

B.Sc., Thompson Rivers University, 2007

A THESIS SUBMITTED IN PARTIAL FULFILMENT
OF THE REQUIREMENTS FOR THE DEGREE

MASTER OF SCIENCE

in

The Faculty of Graduate Studies

(Chemistry)

THE UNIVERSITY OF BRITISH COLUMBIA

(Vancouver)

August 2012

© Laiel Soliman, 2012

ABSTRACT

Current prostate cancer (PCa) diagnosis based on prostate-specific antigen (PSA) has been gradually losing its credibility over the last decade due to contradictory results in published literature and clinical practice. Recently, a group of potential PCa biomarkers in urine, particularly sarcosine, was found to increase significantly as the cancer progressed to metastasis. In Chapter 2, we report a simple, robust, and reproducible capillary electrophoresis–electrospray ionization–tandem mass spectrometry (CE–ESI–MS/MS) method for the determination of sarcosine and other representative potential biomarkers in pooled urine. A solid phase extraction (SPE) technique was optimized for maximum recovery of sarcosine. With no derivatization step, excellent resolution between sarcosine and its isomers (α -alanine and β -alanine) was achieved. A separate non-SPE method was also developed for quantitative determination of highly concentrated urinary metabolites. Precision for intra- and inter-day standard addition calibration of sarcosine were found to be within 15%, whereas intra-day precisions for the rest of the metabolites varied from 0.03 to 13.4%. Acceptable intra-day and inter-day accuracies, ranging from 80 to 124%, were obtained for sarcosine and the other metabolites.

The second part of the thesis takes on a more challenging task. The importance of chiral separation in pharmaceutical, agriculture, and food industries has driven separation scientists to develop more powerful methodologies in conjunction with the structural capabilities of mass spectrometry. In Chapter 3, chiral separation of D- and L-tryptophan was compared on a bare-fused silica capillary and a PEI-coated capillary. Although a higher resolution was observed for uncoated capillaries, analytes were found to migrate slower resulting to longer analysis times ($t_m > 20$ min). With shorter migration times ($t_m < 10$ min)

and acceptable resolution, further investigations on different factors that could affect enantioseparation were conducted on a coated capillary. Highly-sulfated cyclodextrins (HS-CDs), a group of charged CD derivatives, were also utilized for the separation of several racemic amino acids. Resolution with HS-CDs was found to be superior to using native CDs. Unfortunately, due to time constraint, no MS work was presented as the chiral CE/MS work is still currently in progress.

PREFACE

The author has performed all experiments and data analysis in this thesis. She has also written the manuscript for the prostate cancer biomarker research under the helpful guidance and support of Yu Hui, Dr. Amitha Hewavitharana, and Dr. David Chen. Yu Hui helped design the solid phase extraction optimization study and has given the necessary training to the author. The urine samples were obtained from healthy graduate student volunteers at UBC. An ethics approval was not required for this work as the urine samples were obtained anonymously and pooled together to provide a single lot of sample. This work is presented in Chapter 2, which has been recently accepted for publication in *Journal of Chromatography A*:

L.C. Soliman, Y. Hui, A.K. Hewavitharana, D.D.Y. Chen, *J. Chromatogr. A* (2012), <http://dx.doi.org/10.1016/j.chroma.2012.07.021>

TABLE OF CONTENTS

Abstract.....	ii
Preface.....	iv
Table of Contents	v
List of Tables	vii
List of Figures.....	viii
List of Important Terms and Abbreviations	x
Acknowledgements	xi
Dedication.....	xii
Chapter 1: Introduction.....	1
1.1 DEVELOPMENTS IN BIOMOLECULE SEPARATIONS: DEPARTURE FROM TRADITIONAL ANALYTICAL METHODOLOGIES	1
1.2 CAPILLARY ELECTROPHORESIS – ELECTRIC FIELD SEPARATION	3
1.2.1 Transport mechanism.....	3
1.2.2 Electroosmotic flow: a mode of transport.....	5
1.2.3 Capillary coatings	6
1.3 PRACTICAL CONSIDERATIONS ON CE METHOD DEVELOPMENT: DETECTION, IDENTIFICATION, AND CHARACTERIZATION	8
1.4 MASS SPECTROMETRY – THE SEPARATION OF GAS PHASE IONS	10
1.4.1 Electrospray ionization	10
1.4.2 CE–ESI-MS interface	12
1.5 RESEARCH OBJECTIVES	13
1.5.1 Separation of structural isomers: potential prostate cancer biomarkers	14
1.5.2 Separation of optical isomers: chiral amino acids	15
Chapter 2: Monitoring potential prostate cancer biomarkers in urine by capillary electrophoresis – tandem mass spectrometry.....	17
2.1 INTRODUCTION	17

2.2	EXPERIMENTAL	20
2.2.1	Chemicals and reagents.....	20
2.2.2	Preparation of standard stock solutions and buffers	20
2.2.3	Urine sampling and optimized SPE extraction procedure	21
2.2.4	Calibration by standard addition method.....	22
2.2.5	Instrumentation	24
2.3	RESULTS AND DISCUSSION	28
2.3.1	Sarcosine	28
2.3.2	Other metabolites	33
2.3.3	Stability	39
2.4	CONCLUSIONS.....	39
	Chapter 3: Towards chiral separations by capillary electrophoresis mass spectrometry using cyclodextrins as chiral selectors.....	41
3.1	INTRODUCTION	41
3.2	EXPERIMENTAL.....	45
3.2.1	Chemicals and solutions	45
3.2.2	Instrumentation and electrophoretic procedure	46
3.3	RESULTS AND DISCUSSION	47
3.3.1	Separation performance of coated and uncoated capillaries.....	47
3.3.2	Effect of CD concentration on resolution	48
3.3.3	Effects of voltage and capillary length on resolution	49
3.3.4	Effect of organic modifier: methanol.....	51
3.3.5	Derivatized CDs: highly-sulfated cyclodextrins	53
3.4	CONCLUSIONS.....	55
	Chapter 4: Work in progress and future directions.....	56
4.1	CHIRAL SEPARATION WITH CE-ESI-MS	56
4.2	PROSTATE CANCER BIOMARKERS: CLINICAL STUDY PROPOSAL	56
	Bibliography	58

LIST OF TABLES

Table 2-1: Preparation of standard mixtures for the five metabolites by serial dilution.	24
Table 2-2: List of MRM channels and parameters used for the metabolites and their internal standards.....	28
Table 2-4: Summary of results for inter-day (n = 5) and intra-day (n = 3) calibration of sarcosine in pooled urine.....	33
Table 2-5: Intra-day precisions (n = 3) and accuracies of five metabolites by standard addition method of diluted urine. Final concentrations are calculated based on dilutions made during sample preparation.	35
Table 2-6: Summary of intra-day (n = 3) results for non-SPE sample validation.	35

LIST OF FIGURES

Figure 1.1: Schematic diagram of a capillary electrophoresis system with on-line detection..	4
Figure 1.2: The electrical double layer in CE and the formation of electroosmotic flow.	5
Figure 1.3: Illustration of the electrospray ionization process. The evolution of charged droplets via Taylor cone and the formation of gas phase charged analytes as they travel towards the MS inlet.	11
Figure 1.4: Schematic diagram of the CE/MS system and the ESI interface used in the thesis.	12
Figure 2.1: Structures of metabolites including internal standards used in this study.....	19
Figure 2.2: SPE optimization flowchart for pooled urine sample (underlined indicates optimum parameter).	22
Figure 2.3. The multiple reaction monitoring mode used for MS detection.....	27
Figure 2.4: Representative total ion electropherograms (TIEs) and extracted ion electropherograms of (a) native urine and (b) 0.01 mM standard mix. BGE and modifier, 0.4% formic acid, 50% methanol; modifier flow rate, 200 nL min ⁻¹ ; sample in buffer injected at 0.5 psi for 5 s; CE inlet, -30 kV; Needle, 4.5 kV; MS/MS conditions, in Table 2-2 and Section 2.2.5.	30
Figure 2.5. Extracted ion electropherograms of (a) 100-μL SPE native urine sample and (b) Non-SPE 15-fold diluted native urine sample. BGE and modifier, 2.0% formic acid, 50 % methanol; modifier flow rate, 200 nL min ⁻¹ ; sample in buffer injected at 1 psi for 10 s; CE inlet, -30 kV; Needle, 4.5 kV; MS/MS conditions, in Table 2-2 and Section 2.2.5.	37
Figure 3.1: Structures of naturally occurring cyclodextrins: α-CD, β-CD, and γ-CD.	42
Figure 3.2: The counter migration mechanism of anionic highly-sulfated CDs. A ⁺ : analytes; vessels: HS-CDs.....	43
Figure 3.3: Effect of α-CD concentration on the resolution of DL-Trp on a PEI coated capillary. CE conditions: L _T , 60 cm; BGE, 0.18% formic acid, (pH 2.5); -10 kV; capillary temperature, 22 °C; wavelength detection, 214 nm.	49

Figure 3.4: Effect of applied voltage on Rs of DL-Trp on a PEI coated capillary. CE conditions: L _T , 60 cm; BGE, 0.18% formic acid, (pH 2.5); capillary temperature, 22 °C; wavelength detection, 214 nm.	50
Figure 3.5: Effect of adding methanol in BGE on resolution of DL-Trp. CE conditions: L _T , 95 cm; BGE, 0.18% formic acid, (pH 2.5); capillary temperature, 22 °C; wavelength detection, 214 nm; voltage, –10kV.....	52
Figure 3.6: Enantiomeric separation of 0.1 mM DL-Trp, DL-Tyr, DL-DOPA, and DL-Kyn on a bare-fused silica capillary: (a) 5 % HS- α -CD CE, (b) 5 % HS- β -CD, and (c) 5 % HS- γ -CD. CE conditions: L _T , 50 cm; BGE, 0.18 % formic acid, (pH 2.5); capillary temperature, 22 °C; wavelength detection, 200 nm; voltage, 15kV.	54

LIST OF IMPORTANT TERMS AND ABBREVIATIONS

BGE	background electrolyte
CAD	collision activated dissociation
CD	cyclodextrin
CE	capillary electrophoresis
CS	chiral selector
CSP	chiral stationary phase
CUR	curtain gas
CXP	collision exit potential
Da	dalton
DOPA	dihydroxyphenylalanine
DP	declustering potential
DRE	digital rectal examination
EIE	extracted ion electropherogram
EOF	electroosmotic flow
ESI	electrospray ionization
GC	gas chromatography
HPLC	high performance liquid chromatography
HS-CD	highly-sulfated cyclodextrin
ICP	inductively coupled plasma
ID	inner diameter
IS	internal standard
LC	liquid chromatography
LOD	limit of detection
L_t	total length
MRM	multiple reaction monitoring
MS	mass spectrometry
MW	molecular weight
OD	outer diameter
PCa	prostate cancer
PEI	polyethyleneimine
PSA	prostate specific antigen
S/N	signal-to-noise ratio
SPE	solid phase extraction
TIE	total ion electropherogram
UV	ultra-violet

ACKNOWLEDGEMENTS

My dream began with teachers who believed in me: I would like to express my heartfelt gratitude to my wonderful supervisor, Dr. David Chen, for his continuous guidance and support during the course of this program. You inspire your students to aspire. I am also grateful to Dr. Kingsley Donkor and his wife for their endless encouragement throughout these years.

Thank you to my fellow group mates (Roxana, Xuefei, Sherry, Joe, Chang, Cheng, Ju young, Sean, Cai, Matthew, and Marijana) for their valuable inputs, support, and ideas. I will also miss my two very special friends, Alexis and Akram. You made Vancouver a home and research a very enjoyable experience. I will miss our food and hiking trips and of course, our semi-all-nighters in the lab.

I would like to acknowledge the Natural Sciences and Engineering Research Council of Canada for the Postgraduate Scholarship (NSERC CGS M).

Lastly, I would not have been able to do this, if not for my mom's and sister's sacrifice. Thank you for the financial and emotional support. I'll make it up to both of you soon...

To my parents, my first teachers.

Chapter 1: Introduction

1.1 DEVELOPMENTS IN BIOMOLECULE SEPARATIONS: DEPARTURE FROM TRADITIONAL ANALYTICAL METHODOLOGIES

In 1975, DNA sequencing was first attempted by utilizing a gel matrix made of crosslinked polymer or agarose¹. An electrokinetic phenomenon occurs when molecules, under the influence of an electric field, move through the gel at different velocities based on their molecular size and charge-to-mass ratio. This “orthogonality” enables gel electrophoresis to resolve thousands of analytes in a single run. Apart from nucleic acid separation, it has also been widely employed in protein analysis since 1946². However, there are several drawbacks involved in performing gel electrophoresis: (1) laborious gel preparation; (2) manual sampling; (3) exhaustive staining/destaining of analytes on the gel; and (4) long analysis times³. Although there are automated options available today for gel-electrophoresis, it usually leads to additional costs. The birth of electrophoresis in column format has minimized most of the intensive manual labor involved in gel electrophoresis. With the ease in automation, high efficiencies, and small volume sample and buffer requirements, capillary electrophoresis (CE) has evolved into a very powerful tool for analyzing biological samples. Hence after several years, capillary gel electrophoresis (CGE) has begun to contend with gel electrophoresis in the field of DNA sequencing⁴. Yet CGE cannot analyze multiple samples simultaneously nor does it have the exceptional efficiency of the traditional slab gel technique. The first application of capillary array electrophoresis for DNA sequencing was reported in 1990 by Zagurski and McCormick⁵. This application is none other than the revolutionary human genome project which had taken 13 years and 3 billion dollars to complete. Although the price for DNA sequencing has gone down to

\$100,000 per human genome, it is still very expensive⁶. At present, Rech and coworkers⁷ are just among several groups of scientists working towards faster, smaller, and most of all, less expensive DNA (sequencing) microchip electrophoretic devices.

Around late 1990s to early 2000s, the era of genomics was at its pinnacle and the advancement in electrophoretic and chromatographic techniques paved way to more ambitious endeavours. The prevailing need to understand the totality of a system brought subsequent ‘omic’ types of studies including the entire “functional molecular specifications of the genome⁸”, proteomics, and “end products of cellular regulatory processes⁹”, metabolomics. During this period, CE has already established a very successful reputation in DNA sequencing¹⁰. However, the complexity of proteomics and metabolomics demanded more advanced techniques that were capable of not only identifying, but also quantifying enormous numbers of proteins and metabolites. Regrettably, polymerase chain reaction (PCR), the indispensable amplification method exclusive to DNA analysis, cannot simply be adapted to proteins and metabolites. Thus, some laboratories still employ and prefer more primitive methodologies, particularly variants of the popular enzyme-linked immunosorbent assays (ELISA), gel-electrophoresis, and other classical “wet-lab” techniques.

The coupling of mass spectrometry (MS) to one- and two- dimensional separation techniques, both offline and online modes, was certainly a turning point in bioanalytical separations. The last decade has witnessed cutting-edge MS-based research on protein mapping^{11, 12} and metabolomic profiling¹³ that could identify novel phosphorylation sites to characterize biological processes, or discover new disease biomarkers for reliable diagnostics and prognostics tools. With the current trend moving towards high-throughput analysis, shorter analysis times, higher sensitivity, and less instrumentation costs, acceptance for

newer technologies, such as CE and MS, is an imminent future in biomolecular separations. The rest of the chapter provides basic background material for these techniques, namely CE and MS. The theories presented are not meant to be exhaustive, but to provide enough information for readers whose expertise lie elsewhere.

1.2 CAPILLARY ELECTROPHORESIS – ELECTRIC FIELD SEPARATION

1.2.1 Transport mechanism

In basic column chromatography, separation of molecules depends on their individual capacities to partition between the stationary phase and the mobile phase. Molecules that have a higher affinity to the stationary phase tend to move slower compared to molecules that have a higher affinity to the mobile phase. Thus, the term *retention time* is used to describe the amount of time the molecules are ‘retained’ in the stationary phase. On the other hand, separation in CE occurs inside a narrow-bore capillary filled with a suitable background electrolyte (BGE) or buffer. A plug of sample is injected at the capillary inlet and a high voltage, usually up to a maximum of 30 kV, is applied on one of the chemically inert (*e.g.*, platinum) electrodes immersed in buffer reservoirs located at each end of the capillary. An online detector is placed near the outlet by removing a section of the polyimide coating to serve as an optical viewing ‘window’. An electropherogram is generated by plotting the acquired signal versus the *migration time* or the time it takes for each analyte to reach the detector. Figure 1.1 shows the schematic diagram of a capillary electrophoresis system.

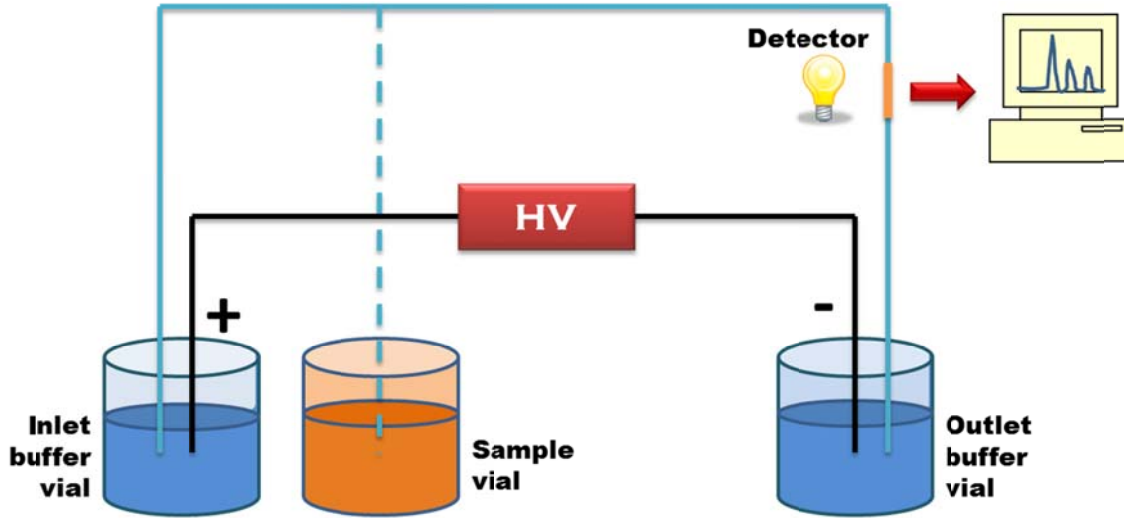


Figure 1.1: Schematic diagram of a capillary electrophoresis system with on-line detection.

Analytes migrate in separate zones under the influence of an electric field, based on their individual electrophoretic mobilities. The electrophoretic mobility (μ_{ep}) of an analyte depends on its charge-to-size ratio and the viscosity of the buffer solution. It is expressed as:

$$\mu_{ep} = \frac{q}{6\pi\eta r} = \frac{v_{ep}}{E} \quad (1-1)$$

where q and r are the effective charge and radius of the analyte, respectively, and η is the viscosity of the buffer. The actual speed or electrophoretic velocity (v_{ep}) of an analyte is related to its mobility and the electric field strength, E . Field strength is obtained by dividing the applied voltage with the total length of the capillary, L_t . The electrophoretic velocity, v_{ep} , can be measured experimentally:

$$v_{ep} = \frac{L_d}{t_m} \quad (1-2)$$

where L_d is the length of the capillary from the point of injection to the detection window, and t_m corresponds to migration time of the analyte.

1.2.2 Electroosmotic flow: a mode of transport

The apparent electrophoretic mobility of each analyte can be in fact the sum of two contributions: the inherent electrophoretic mobility of the ion, and the electroosmotic flow mobility (μ_{eof}) of the bulk solution. The electroosmotic flow (EOF) is one of the fundamental fluid transport mechanisms in CE. A fused silica capillary has ionizable silanol groups on its inner surface. If the capillary is rinsed with a basic electrolyte solution, for example a buffer with $\text{pH} > 9$, a complete dissociation of the silanol groups occurs inducing the formation of two distinct regions inside the capillary. The cations in the buffer are immediately attracted to the negatively-charged wall generating a “fixed layer” which is sometimes called the *Stern* layer, as shown in Figure 1.2. As the name implies, the fixed layer is quite rigid and mainly composed of positively charged ions. As the distance from the capillary wall increases, the electric potential experienced by the subsequent diffuse layer falls exponentially. The residual potential from the excess negative charges at the capillary wall at the start of the diffuse layer is called the zeta potential (ζ).

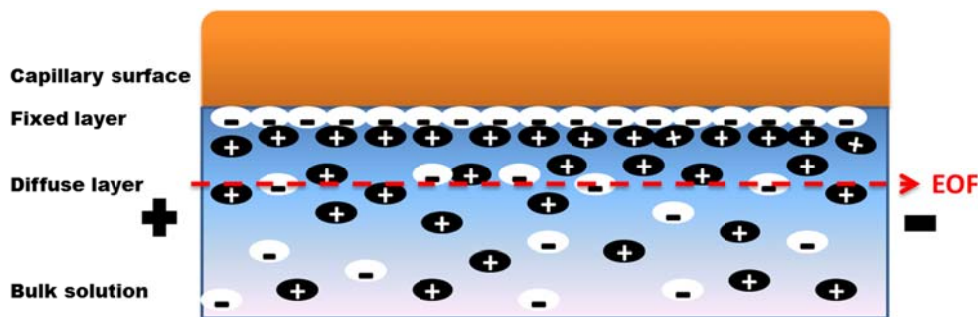


Figure 1.2: The electrical double layer in CE and the formation of electroosmotic flow.

If a positive voltage is applied on the inlet electrode (normal polarity), the hydrated cations in the diffuse layer migrate toward the negatively-charged electrode (cathode) carrying the bulk

solution to move in the same direction. The diffuse layer is the driving force of EOF and it contains more cations than anions. The EOF mobility (μ_{eof}) is directly proportional to the dielectric constant (ε) of the BGE, the zeta potential of the capillary wall (ζ), and the field strength (E). It is also inversely proportional to the viscosity of BGE.

$$\mu_{eof} = \frac{v_{eof}}{E} = \frac{\varepsilon\zeta}{4\pi\eta} \quad (1-3)$$

By taking into account the mobility of EOF, the apparent net mobility (μ_a) of an ion during CE separation is therefore the vector sum of electrophoretic mobility of the analyte and the EOF mobility.

$$\mu_a = \mu_{ep} + \mu_{eof} \quad (1-4)$$

The EOF is directly related to the properties of the buffer such as pH, ionic strength, and viscosity. Therefore, by exploiting any of these properties, the selectivity of a particular separation can be modified. Under normal polarity, EOF flows from anode to cathode. Positively-charged ions will migrate at a faster rate than EOF. Neutral molecules will travel at the same rate as EOF. If the magnitude of EOF mobility is significantly larger than the individual electrophoretic mobilities of the anions, which is usually the case, the anions too will eventually migrate toward the cathode although at a slower rate.

1.2.3 Capillary coatings

Proteins and other large biomolecules containing multiple sites of positively-charged species in their structures may adsorb strongly to the negatively-charged capillary wall. Hjertén believed that the simplest way to overcome this obstacle is to eliminate EOF. He derived the mobility equation of EOF, μ_{eo} , which is shown below¹⁴:

$$\mu_{eo} = \frac{\varepsilon}{4\pi} \int_0^{\zeta_{eo}} \frac{1}{\eta} \cdot d\psi \quad (1-5)$$

where ζ_{eo} is the zeta potential of the tube wall and ψ is the electric potential. According to the equation, EOF is suppressed when the viscosity of the bulk solution approaches infinity; thus, the value of the integral is zero. Hjertén was able to deactivate the silanol groups through covalent bonding with highly viscous polymers such as methylcellulose and linear polyacrylamide compounds. Permanent coating eliminates analyte-wall interactions during separation. The coating procedure usually consists of three steps: pretreatment of the wall for activation, double bonds introduction to the wall, and binding of the polymer¹⁵. Neutral coatings almost completely eliminate EOF and many of these are now commercially available through companies who also manufacture CE instruments. However, in this thesis, a positively-charged coating was employed for the analysis of cationic analytes. The polyethyleneimine (PEI) coating procedure is outlined in US Patent 6923895 B2. The procedure was slightly modified in my experiment to shorten the coating time. The positively-charged capillary wall reverses the EOF's flow to the anode and also prevents the adsorption of cationic analytes. The fast anodic EOF requires a negative voltage application on the inlet to ensure that the analytes are still detected on the outlet of the CE system.

An alternative to permanent deactivation of the silanol groups is to add a viscous polymer in the buffer. The adsorption of the buffer additive to the capillary wall may not entirely abolish EOF, but it can slow it down enough to achieve a similar purpose. Contrary to static coating, “dynamic coating” is obtained by rinsing the wall with the buffer additive. Instead of buying more expensive, readily coated capillaries, dynamic coating allows the use of less expensive fused silica capillaries and avoids undergoing strenuous coating procedures.

However, since the coating is based on adsorption, regeneration of the coating is necessary to prolong its lifetime and obtain reproducible analysis runs.

1.3 PRACTICAL CONSIDERATIONS ON CE METHOD DEVELOPMENT: DETECTION, IDENTIFICATION, AND CHARACTERIZATION

In contrast to gel electrophoresis, the band broadening effect in CE caused by Joule heating is minimal. The generation of heat as a consequence of frictional forces between ions and solute molecules can lead to the formation of a temperature gradient. With larger surface area-to-volume ratio, heat is dissipated more effectively in capillaries than in slab gels. This permits the use of higher voltages to obtain more efficient separations. Hence it is no surprise that CE has superior separation efficiencies ($N \approx 10^5 - 10^6 \text{ m}^{-1}$ or higher) compared to other chromatography techniques such as GC ($N \approx 3 \times 10^3 \text{ m}^{-1}$) and HPLC ($N \approx 10^5 \text{ m}^{-1}$)¹⁶.

An advantage of using CE in biological analysis is that there is no need for derivatization. As a gas phase separation technique, GC often takes the derivatization route to chemically modify non-volatile biological compounds to improve their stability and compatibility in GC analysis¹⁷. This is easily circumvented in CE, since traditional CE occurs in aqueous matrix. Whereas HPLC is still the primary analytical technique of choice today for most laboratories, CE has become a reliable complementary tool in bioanalytical research and pharmaceutical industries. For some analytes that are unresolvable in HPLC, they can easily be separated in CE.

Amidst these advantages, CE suffers greatly from low detection sensitivity when using the standard optical detection modes (e.g., UV-vis). Short optical path lengths for

online type detectors, very small capillary diameters, and limited loading capacity all contribute to poor concentration limits of detection (LODs). Nevertheless, UV-vis is still the least expensive and most common detection mode for commercial CE instruments. Thus, by utilizing high intensity lamps with accompanying wavelength filters, affordable and simple CE analysis can still be achieved. Alternative sensitive modes of detection are also available including laser-induced fluorescence (LIF), conductometry, and amperometry¹⁸.

The complexities of proteomic and metabolomic studies demand for a more powerful CE detector. The possibility of coupling CE to mass spectrometry creates a complementary separation dimension. According to Giddings' theory of separation, the peak capacity of a system in two dimensions is not the sum— rather, it is the product of the individual peak capacities of each dimension¹⁹. In addition to improved resolution, MS offers valuable structural information and identification of the components of a complex sample mixture. These features are often employed to deduce amino acid sequence information, post-translational modifications, phosphorylations and more. LC/MS and GC/MS may perhaps continue to dominate the market for commercial analytical instrumentation; after all, they have a history of more than 50 years of development. But the emergence and rapid development of powerful CE/MS interfaces²⁰ in combination with electrospray ionization (ESI), has made CE a complementary analytical tool in this 'omics' period of our generation. The next section will only examine relevant mass spectrometry fundamentals used in this study. There are excellent MS textbooks²¹⁻²³ published recently which offer additional information and in-depth reading.

1.4 MASS SPECTROMETRY – THE SEPARATION OF GAS PHASE IONS

CE/MS represents a two-dimensional separation process with MS as the second dimension. In MS, analytes are separated based on their mass-to-charge ratios. But in order to effectively couple CE to MS, the sample must be introduced to MS as gaseous charged ions. This explains the early development of combining GC to MS since both separation techniques occur in gaseous phase. Nonetheless, one must realize the challenges involved in coupling a liquid-based separation (CE) to a gas phase one (MS). There are two approaches available for CE/MS analysis. The first one is an offline mode which collects the sample from the CE system after separation and injects it to the MS separately. It offers the user a choice between different types of ion sources and allows individual optimizations of the CE and MS systems²⁴. However, offline modes commonly employ fraction collectors which dilute analyte concentrations by mixing the eluted sample with a buffer solution in the collection reservoirs²⁵. The second approach is an online mode where the analytes are transported directly from CE to MS *via* an interface. The online mode has minimum sample handling compared to the offline mode, which reduces the possibility of sample loss and contamination. At present, the most popular commercially available CE/MS interfaces are based on electrospray ionization (ESI) because it provides higher ionization efficiency, and allows the detection of larger multiply-charged biomolecules²⁶.

1.4.1 Electrospray ionization

Electrospray ionization (ESI) is a technique that generates gaseous ions at atmospheric pressure directly from a solution by spraying the sample into a high electric field region. In 1988, Fenn and co-workers²⁷ reported ESI mass spectra of multiply-charged intact proteins with MWs in the range of 5,000 – 40,000 Da. By being able to ionize large, non-

volatile, and intact biomolecules, his ground-breaking work on ESI won him a Nobel Prize in 2002. The mechanism of ESI is illustrated conceptually in the diagram below:

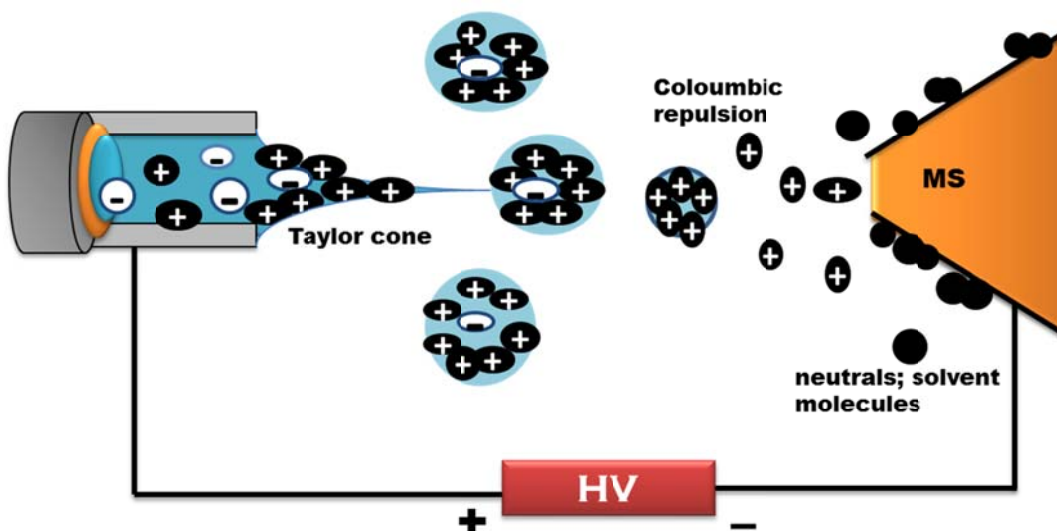


Figure 1.3: Illustration of the electrospray ionization process. The evolution of charged droplets via Taylor cone and the formation of gas phase charged analytes as they travel towards the MS inlet.

A positive (or negative) voltage of 2 – 5 kV, also known as the ESI voltage, is applied on the ESI needle. At the tip of the needle, a so-called “Taylor cone” forms as a result of sample solution being pulled by the potential difference between the needle and the MS inlet. A liquid filament is then ejected from the Taylor cone generating charged droplets which are made possible by the electrical contact between the background electrolyte and the ESI needle. The initial size reduction of the droplets is due to solvent evaporation, sometimes aided by a drying gas such as nitrogen. The sizes of these droplets continue to shrink until the electrostatic force of the surface charges overcomes the cohesive forces of the solvent, also known as the Rayleigh limit. When this limit is reached, Coulombic fission occurs

forming “offspring” droplets. The process of solvent evaporation alternates with Coulombic repulsion so that in the end, charged analytes devoid of solvent enter the MS orifice.

1.4.2 CE-ESI-MS interface

As ESI is the most important *atmospheric pressure ionization* (API) technique for interfacing solution-based separations with MS, it is also the primary choice for both HPLC/MS and CE/MS hyphenations. At atmospheric pressure, the enthalpy required to evaporate the solvent is satisfied. The collision of ambient air with charged droplets causes the rate of desolvation to go up as a result of the increased thermal energy of the solvent molecules. The CE-ESI source depicted in Figure 1.4 differs from commercially available ESI interfaces and is constructed by our group²⁸.

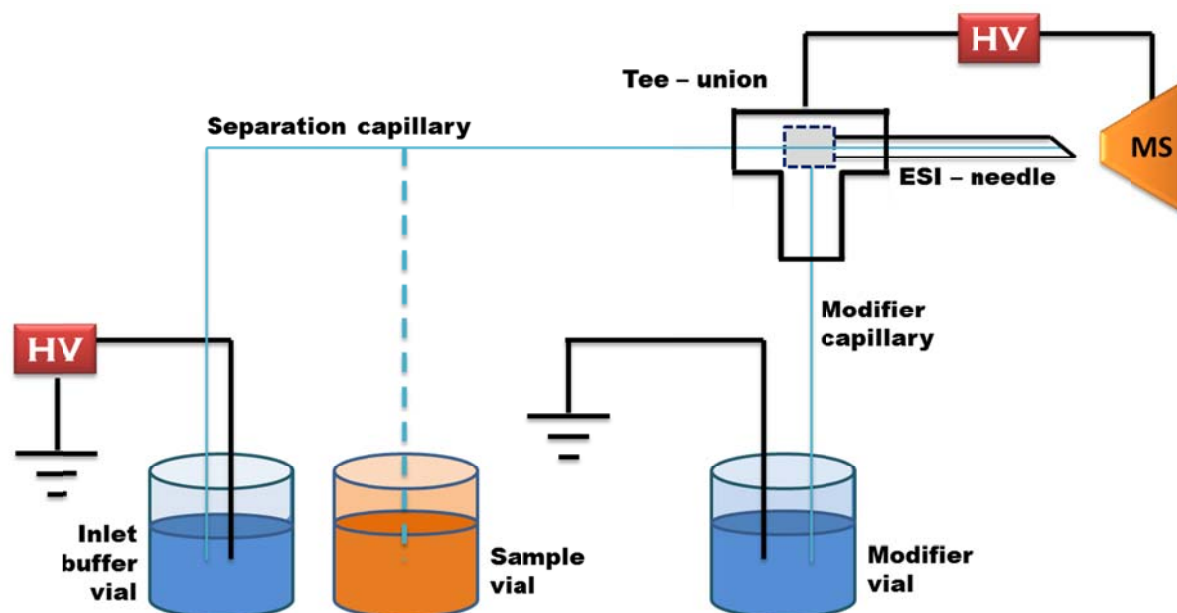


Figure 1.4: Schematic diagram of the CE/MS system and the ESI interface used in the thesis.

An excellent review of CE–ESI interfaces can be found elsewhere [18]. Online coupling of CE to MS requires the outlet capillary to be directly connected to the ion source of MS. Removal of the outlet vial requires a means of establishing a stable electrical contact with the MS as well as providing a terminal electrode for CE. The design in Figure 1.4 is developed in our group²⁸ and it uses a flow through micro vial strategy to minimize the common dilution problem encountered with sheath-liquid ESI interfaces. The separation capillary is fully inserted into a stainless steel needle with a bevelled tip. Another capillary is inserted at the orthogonal entrance of the tee-union to deliver a chemical modifier solution typically composed of volatile organic solvents such as acetonitrile, methanol, and isopropanol. The modifier solution meets the separation BGE at the capillary end and the emitter tip, creating a flow through micro-vial to act as the outlet vial of CE and the terminal electrode. Oftentimes, the nanospray flow-rate of CE may not provide a stable ESI spray but this is alleviated by adjusting the modifier flow-rate using the CE system itself or an external syringe pump. By adding volatile acidic or basic components to the modifier such as formic acid, ammonium acetate, or acetic acid, compatibility of the CE effluent and the ionization efficiency of the analyte can also be improved.

1.5 RESEARCH OBJECTIVES

The main objective of this thesis is to demonstrate the feasibility of CE and MS in the separation and quantification of important biological isomeric compounds. It is divided into two sub-objectives which are further discussed in the following sections.

1.5.1 Separation of structural isomers: potential prostate cancer biomarkers

The first part of this thesis is focused on the analysis of structural or geometrical isomers, specifically the isomers of alanine: sarcosine, α -alanine (α -Ala), and β -alanine (β -Ala). The three isomers are all naturally occurring amino acids in the human body, mainly found in muscles and tissues. α -Ala and β -Ala have shown detectable levels in urine^{29, 30}, blood^{31, 32}, and cerebrospinal fluid^{31, 32}. On the other hand, sarcosine is a by-product and intermediate compound during glycine's synthesis and degradation³³. It is normally detected in urine and blood³³.

Recently, sarcosine and other amino acids: namely, cysteine, leucine, glutamic acid, kynurenine, and proline, were identified as potential prostate cancer biomarkers in urine³⁴. The endogenous level of sarcosine is extremely low in comparison to α -Ala's and β -Ala's concentrations in unprocessed urine and plasma. Thus, it is essential to have a baseline resolution, or better, between sarcosine and its isomers before performing any quantitative analysis. Sarcosine is found to coelute with α -Ala in HPLC/MS analysis unless a chemical derivatization is carried out to improve the selectivity between the two analytes³⁵. Likewise, GC/MS must also employ derivatization to increase the volatility of amino acids or any other polar compounds for GC analysis. Derivatization is an additional step in the analytical process which can significantly lengthen the overall analysis time. Reaction efficiency, stability of the derivatizing reagent, matrix compatibility of the labeling chemistry, and possible interference of unreacted reagent must also be considered when taking the derivatization route. Chapter 2 of this thesis describes the development of a CE-ESI-MS method that allows the separation of sarcosine from its isomers and the detection of other metabolites in urine. Due to its low endogenous level, an optimized solid phase extraction

procedure was designed to maximize the recovery of sarcosine from urine, and preconcentrate sarcosine to a detectable level.

1.5.2 Separation of optical isomers: chiral amino acids

A chiral molecule lacks an internal plane of symmetry and has a non-superimposable mirror image. Enantiomers, a pair of chiral compounds, often have identical physical properties such as boiling points, solubility, and UV and IR spectra. They cannot be differentiated by conventional chemical characterization methods. The only way to distinguish between a set of enantiomers is through their selective behaviour in the presence of a chiral environment. The importance of stereoisomerism in biological activities can easily be understood if we consider the mechanisms involved when a drug interacts with its target. The usual benefits (or harmful effects) of a drug are only manifested after it selectively binds itself with receptors or enzymes, which generally requires a three-dimensional fit³⁶. Many pharmaceutical drugs, agricultural pesticides, and industrial chemicals possess one or more chiral centres. In the past, these drugs were marketed as racemates and in most cases, no information about the individual properties of each enantiomer was available³⁶. Today, strict international regulations exist on the production of chiral drugs due to the importance of optical isomerism in pharmacodynamic and pharmacokinetic behaviours of enantiomers³⁷⁻³⁹. Stringent guidelines are necessary to avoid recurrence of horrific accidents such as the infamous thalidomide tragedies in the 1960s⁴⁰.

The efforts in separating racemic mixtures were amplified when scientists realized that it was less expensive and more practical than synthesizing optically pure compounds which required enantiomerically pure starting reagents. Whether for pharmaceutical or

quality control purposes, there are a number of different techniques employed for preparative and analytical type separations. The classical and more intuitive scheme is to simply react a racemic mixture with an optically pure reagent to produce a pair of diastereomers. These diastereomers will have different physical properties; hence they can be separated using conventional methods. This process is tedious, especially for preparative analysis, as the diastereomers will have to be converted back to their respective enantiomers after the separation step. The risk of racemization taking place during conversion and retrieval processes is also a serious concern.

A more elegant strategy is to separate enantiomers by forming transient diastereomers during the liquid phase separation step. Addition of chiral selectors in the stationary or mobile phases in chromatography (or BGE in CE) creates the necessary chiral environment. Some chiral selectors (CSs) or chiral stationary phases (CSPs) are suitable for a broad spectrum of compounds. The selectivity and specificity of a particular CS or CSP depend on the type and structures of the molecules being studied. Unfortunately, the existence of a universal chiral selector for any enantiomers remains to be discovered.

In Chapter 3, we have selected a few amino acids to study a group of CSs in CE. We investigated several parameters that could affect the resolution of these enantiomeric pairs. The scope of this chapter is purely exploratory.

Chapter 2: Monitoring potential prostate cancer biomarkers in urine by capillary electrophoresis – tandem mass spectrometry

2.1 INTRODUCTION

In 2011, a recorded number of 266,390 men in North America were diagnosed of prostate cancer (PCa), and 37,820 died from the disease^{41, 42}. This year, the number of diagnoses and deaths is projected to be greater than last year and will steadily increase according to SEER Cancer Statistics Review⁴¹. Prostate-specific antigen (PSA), initially believed to be a protein specific to prostate, is the first PCa biomarker approved by the FDA for diagnosing PCa along with a digital-rectal examination (DRE)⁴³. However, controversies surrounding cancer-free patients who suffered consequences of unnecessary treatment due to their elevated PSA levels have stimulated active studies disputing the validity of PSA blood tests for PCa screening⁴⁴. Particularly, its weakness in discriminating between benign prostatic hypertrophy (BPH) and malignant PCa in patients with PSA levels of 4 – 10 ng mL⁻¹ has led to several false-positive and false-negative results. Therefore, the search for effective, non-invasive diagnostic tools and new biomarkers for PCa is of paramount importance for the whole cancer research community^{45, 46}.

Cancer progression, accompanied by highly complex molecular processes in the human body, can alter the whole metabolome of an organ. Metabolome refers to the full complement of small-molecule intermediates and products during metabolism of a living organism. One reason for the controversies surrounding well-recognized single-molecule biomarkers, such as PSA for PCa, is that often an accurate diagnosis based on a single biomarker is limited by its inherent sensitivity and specificity. Metabolomic strategies in

studying diseases have increasingly become popular in the last few years^{47, 48}. By generating metabolomic profiles for patients at different stages of the disease, a similar pattern for a group of molecules can be recognized for patients at the same stage of cancer.

Following this rationale, Sreekumar et al.³⁴ profiled 1,126 metabolites in tissue, plasma, and urine of PCa patients in order to screen for possible biomarkers. Their multi-marker approach narrowed down their list of potential biomarkers to 124 metabolites that can help to distinguish between benign, localized, and metastatic PCa. Sarcosine, an N-methyl derivative of glycine, took the spotlight by displaying dramatic increase in concentration from benign to metastatic PCa in tissue and urine. Their study was then immediately followed by a multitude of others who either questioned or supported their findings⁴⁹⁻⁵⁶. Furthermore, several communication reviews and letters to the editor poured in⁵⁷⁻⁵⁹ to scrutinize the contradictory results from published literature. Many of these letters have criticized the ambiguity in methodology, sample collection, data analysis and lack of, or incomplete, validation process. At the time of writing our paper, the answer to the question of whether sarcosine is or is not a biomarker for PCa is yet to be established.

Sensitivity and specificity of a method can be vastly improved by combining the predictive power of each marker. In this work, we considered it redundant to analyze thousands of small molecules and regenerate metabolomic profiles for PCa patients as this grueling task was already undertaken by Sreekumar et al.³⁴. Instead, we selected six metabolites (Figure 2.1) from their results including sarcosine, L-proline, L-cysteine, L-leucine, L-glutamic acid, and L-kynurenine, which showed significant increases during cancer progression, and showed the feasibility of a multimarker strategy for prostate cancer diagnosis.

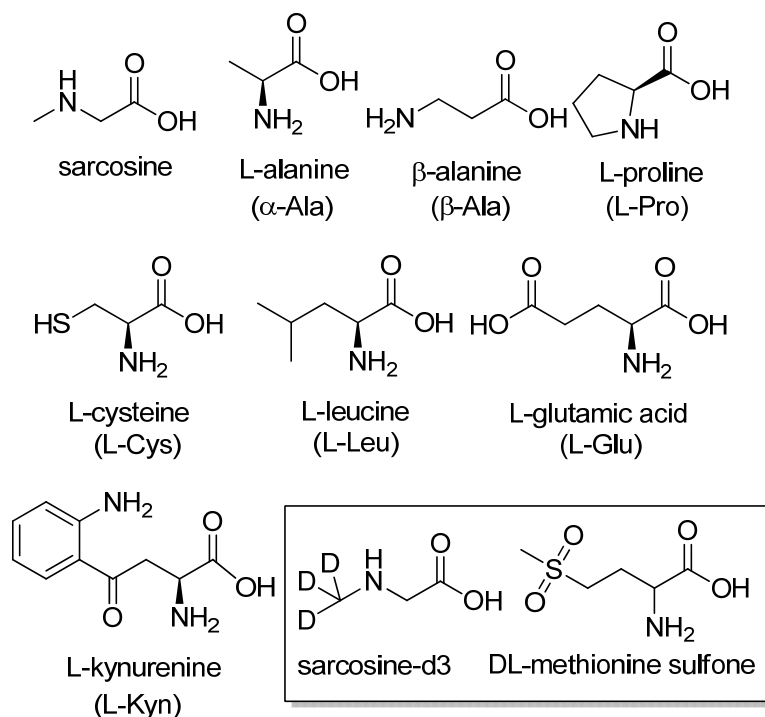


Figure 2.1: Structures of metabolites including internal standards used in this study.

We report the first quantitative CE–MS/MS method to analyze sarcosine and a group of other potential PCa biomarkers in urine using a newly developed CE-ESI-MS interface in our group²⁸. Others have attempted to use CE/MS to profile the metabolome of urine^{60, 61}; however, here we offer a practical, robust, and reproducible method ready for prospective PCa biomarker screening. This protocol can be modified to accommodate many other urinary metabolites if necessary.

The method includes an optimized solid phase extraction (SPE) procedure (Section 2.2.3) for low level analytes (e.g., sarcosine) and does not require a derivatization step unlike existing LC/MS or GC/MS protocols^{62, 63}. For quantifying more concentrated metabolites in urine, we demonstrate that no extraction is necessary and simple dilution of the sample is sufficient for CE/MS analysis. Clinical samples were not used in this study because the

scope of this study was to develop and validate a reliable analytical method for the measurement of multimarkers for PCa. We intend to use these methods to conduct a clinical investigation in collaboration with clinicians, following ethics approval.

2.2 EXPERIMENTAL

2.2.1 Chemicals and reagents

All metabolite standards with minimum of 98% purity were purchased from Sigma Chemical Co. (St. Louis, MO). Internal standards, sarcosine-D₃·hydrochloride and L-methionine sulfone, were obtained from Toronto Research Chemicals Inc. (North York, ON, Canada) and Sigma Chemical Co., respectively. Formic acid (88%), NaOH, HCl, methanol (HPLC grade), and glacial acetic acid were purchased from Fisher Scientific (Nepean, ON, Canada). Reagent grade picric acid (98%, 35% water) for creatinine analysis was also obtained from Sigma Chemical Co. (St. Louis, MO). PEI coating reagent of trimethoxysilylpropyl-modified polyethylenimine, 50% in isopropanol was purchased from Gelest Inc. (Morrisville, PA).

2.2.2 Preparation of standard stock solutions and buffers

Stock solutions of sarcosine (1000 µM), L-alanine (1000 µM), β-alanine (1000 µM), L-proline (1000 µM), L-cysteine (1000 µM), L-glutamic acid (2000 µM), L-kynurenine (200 µM), and L-methionine sulfone (1000 µM) (Figure 2-1) were prepared in deionized 18 MΩ water. The internal standard (IS), sarcosine-D₃ (7.78 mM) was also prepared in deionized 18 MΩ water, divided into 5 aliquots and stored at -20 °C. All stock solutions and buffers were

filtered through 0.22- μ m sterile, Nylon syringe filters and stored at 4 °C in a refrigerator unless otherwise stated.

2.2.3 Urine sampling and optimized SPE extraction procedure

Urine samples were obtained from 20 healthy volunteers between the ages of 23 to 30 years. The pooled urine sample was divided into 1 mL aliquots and stored at -20 °C.

The solid phase extraction (SPE) procedure for urine was optimized (Figure 2.1) for 100 μ L urine sample spiked with 20 μ L 0.01 mM sarcosine standard and 20 μ L 0.01 mM IS. The optimized SPE procedure was as follows: a 100- μ L urine sample was treated with 350 μ L of 0.1 M acetic acid and spiked with the sarcosine standard and IS prior to extraction. The SPE cartridge, a 30-mg Strata-X strong cation mixed mode cartridge from Phenomenex (Torrance, CA) was equilibrated and conditioned with 1 mL methanol and 1 mL 0.1 M acetic acid, respectively. The treated urine sample was then loaded into the cartridge and drained first by gravity followed by positive air pressure application. Successive washings of 0.5 mL acetic acid (0.01 M) and 0.5 mL methanol were applied under a gentle flow of positive air pressure. The cartridge was then dried with air for 1 min before eluting twice with 350 μ L of methanol/ammonium hydroxide (15:85) solution under gravity and positive air pressure. The combined eluted samples (700 μ L) were concentrated using an Eppendorf Vacufuge™ and the residue was reconstituted in 20 μ L buffer. The reconstituted sample was filtered through 0.45- μ m Costar® Spin-X centrifuge tube filter (Corning, NY) at 13,200 rpm for 30 s prior CE/MS analysis.

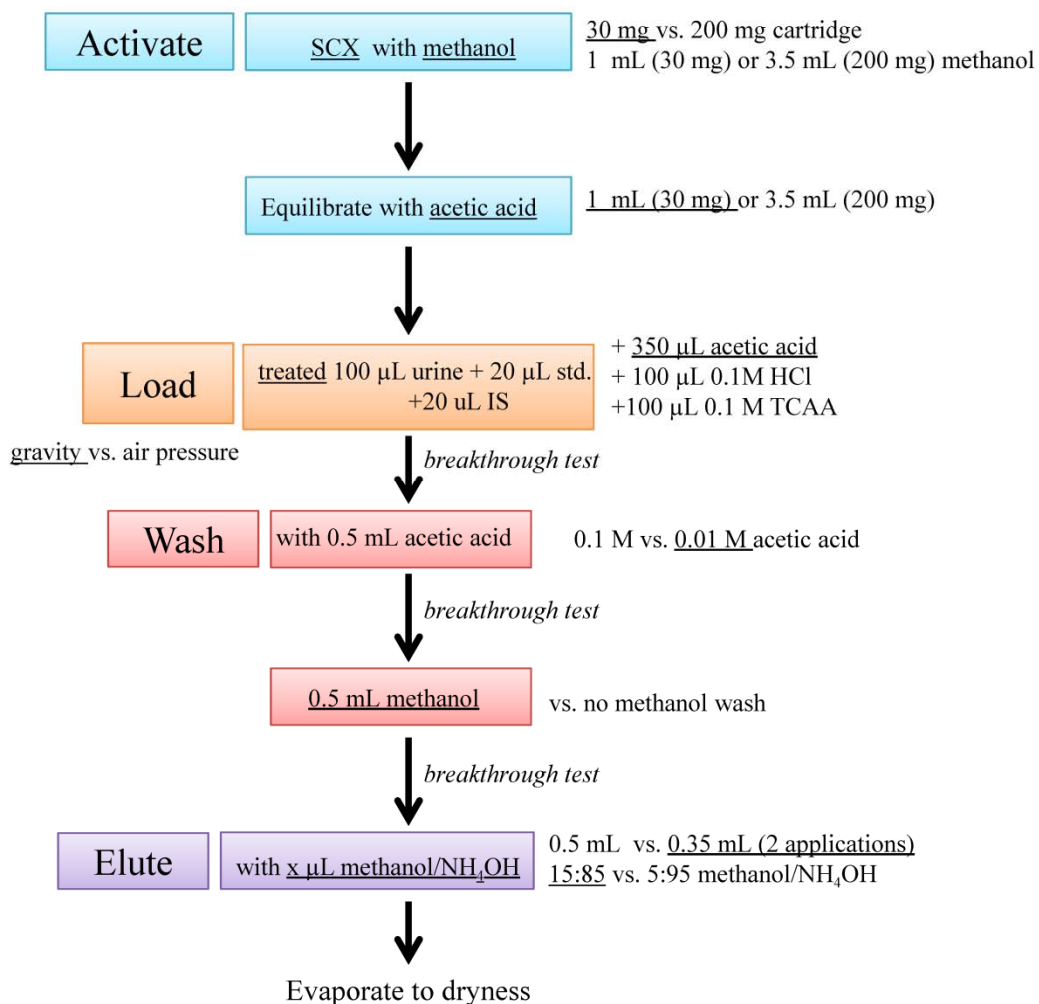


Figure 2.2: SPE optimization flowchart for pooled urine sample (underlined indicates optimum parameter).

2.2.4 Calibration by standard addition method

- Sarcosine*

Calibration standards of 0.50, 1.00, 2.50, 5.00, 10.00, and 20.00 µM sarcosine were prepared by diluting 100 µM sarcosine with deionized 18 MΩ water. The IS stock solution of sarcosine-D₃ was also diluted with deionized 18 MΩ water to give a 10 µM working

solution which was divided into 1 mL aliquots and stored at $-20\text{ }^{\circ}\text{C}$. A calibration curve was generated by adding 20 μL of each calibration standard and 20 μL IS into a 100 μL urine sample prior to SPE extraction. Blank samples were also prepared by substituting the standard volume of 20 μL with deionized water.

- *Other metabolites*

Extremely high endogenous levels of L-Pro, L-Cys, L-Leu, L-Glu, and L-Kyn in the pooled urine sample were found to saturate the MS detector after SPE extraction/pre-concentration step; thus, a separate method was developed for analytes that were present at high concentrations in native urine. Calibration standard mixtures of 0.625–20.0 μM for L-Pro, 3.125–100 μM for L-Cys, 2.50 – 80.0 μM for L-Leu, 3.125–100 μM for L-Glu, and 0.125–4.00 μM for L-Kyn were prepared by serial dilution in BGE from their corresponding stock solutions. The pooled urine sample was filtered through Amicon® Ultra-15 5 kDa Centrifugal Filter Units (Billerica, MA) in a Sorvall swinging bucket rotor at 4000 G for 20 min at around $15\text{ }^{\circ}\text{C}$. The standard addition calibration curve was constructed by combining 191 μL of each standard mixture listed in Table 2-1 with 5 μL of IS (200 μM) and 14 μL of filtered urine. These volumes were chosen to yield a final dilution factor of 15 for the urine sample. Blank samples were also prepared by substituting the standard volume of 191 μL with deionized water. The concentrations of the standard mixtures are listed in Table 2-1.

Table 2-1: Preparation of standard mixtures for the five metabolites by serial dilution.

Analyte	Standard mixture (μM)					
	1	2	3	4	5	6
L-Pro	0.625	1.25	2.5	5	10	20
L-Cys	3.125	6.25	12.5	25	50	100
L-Leu	2.50	5.00	10	20	40	80
L-Glu	3.125	6.25	12.5	25	50	100
L-Kyn	0.125	0.25	0.5	1	2	4

- *Creatinine*

Concentrations of endogenous metabolites in urine can fluctuate between different individuals depending on water consumption and physiological factors. However, the formation of creatinine in the human body is set at a relatively constant rate⁶⁴. Hence, the concentration of creatinine is commonly used to normalize the concentrations of other metabolites in urine. A Jaffe reaction⁶⁵ based assay on a 96-well plate was employed using a saturated alkaline picrate solution to produce a yellow complex with creatinine. The samples were analyzed by visible light absorption at the characteristic wavelength using a Beckman Coulter DTX880 multimode reader set at 450 nm.

2.2.5 Instrumentation

- *CE/MS system and software*

Some optimizations and qualitative analyses were performed on a P/ACE MDQ capillary electrophoresis system (Beckman Coulter, Brea, CA) coupled with a Finnigan LCQ*DUO ion trap mass spectrometer (Thermo Scientific, Waltham, MA). All calibration experiments were carried out on a PA800 plus capillary electrophoresis system (Beckman Coulter, Brea, CA) connected to an AB SCIEX API 4000 triple quadrupole mass spectrometer (AB SCIEX, Framingham, MA). Nitrogen (UHP) was used as curtain and

collision gas. A modified commercial capillary cartridge built for CE/MS and a homemade ESI interface developed in our group were utilized for all experiments. The schematic is shown in Chapter 1 (Figure 1.4). The needle tip was positioned 1–2 cm from the front of the heated capillary inlet or curtain plate orifice. It is possible to control the temperature of the CE/MS cartridge by employing a liquid coolant, but it was not used in this particular application because the current generated in CE at the voltage used was less than 8 μ A. Thus, heat generated in the CE operation is minimal. All data acquisition, system control, and integration were performed with Analyst® 1.4.2 software (AB SCIEX, Framingham, MA).

- *Electrophoretic procedure*

CE separations were carried out on a 50- μ m inner diameter (ID) \times 365- μ m outer diameter (OD) \times 85 cm length (L_T) fused silica capillary (Polymicro Technologies, Phoenix, AZ) coated with cationic PEI. A chemical modifier was introduced through a 75- μ m (ID) \times 365- μ m (OD) \times 80 cm (L_T) bare fused silica capillary set at 200–250 nL min⁻¹ flow rate. The concentrations of formic acid and methanol, the components of background electrolyte (or separation buffer), were varied methodically to give the best compromise between sensitivity, resolution, and analysis time. The modifier was also optimized by changing the formic acid and methanol composition. When the separation buffer and modifier solution had the same composition, the most stable and sensitive ESI was achieved. Therefore, the same solution was used for separation and flow rate modification throughout all the experiments.

For sarcosine analysis, 0.4% formic acid in 50% methanol was found to give the fastest analysis time with good baseline resolution ($R_s > 1.5$) from α -Ala and β -Ala. At the start of the day, the modifier and separation capillaries were rinsed with BGE for 10 min at

40 psi. The sample was injected at 0.5 psi for 5 s. The separation and modifier capillaries were then immersed in the buffer vials and a voltage of –30 kV was applied. Before each injection, the separation capillary was rinsed with buffer for 3 min at 40 psi.

Simultaneous separation of other metabolites required a higher formic acid percentage (2%) with the same methanol composition (50%). The sample was injected at 1 psi for 10 s and a voltage of –30 kV was applied. Between injections, it was crucial to rinse the separation capillary at 40 psi with methanol for 5 min, air for 1 min, and buffer for 5 min as the migration would slow down significantly without these steps. Without SPE, the presence of anionic analytes in the sample may adsorb on the capillary wall which can lead to changes in the electroosmotic flow.

- *Tandem mass spectrometry*

The multiple-reaction monitoring (MRM) method was developed manually instead of using the instrument's built-in auto-optimization feature to ensure reproducibility and accuracy. In MRM mode, ions were preselected in the first quadrupole (Q1) which were then fragmented by collisional induced dissociation (CID) with nitrogen gas in the second quadrupole (Q2). Unique fragment ions corresponding to individual precursor ions were selectively allowed in the third quadrupole (Q3) to pass the detector.

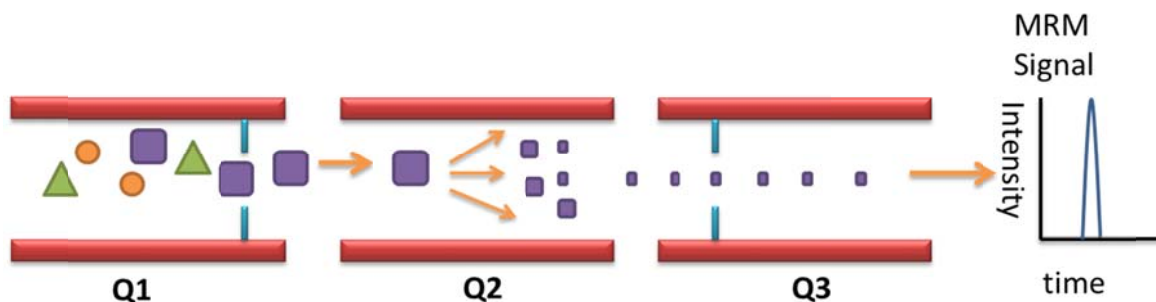


Figure 2.3. The schematic of multiple reaction monitoring mode used for MS detection.

Separation independent MS/MS parameters were optimized by directly infusing 10 μM of individual analytes in background electrolyte. A Q1 scan on positive ion mode was first performed over a 2 amu width of the particular analyte to optimize the declustering potential (DP) and identify the exact mass of the $[\text{M}+\text{H}]^+$ ion in the spectrum. The DP parameter helps in minimizing solvent cluster ions attached to the sample. There is a risk of ion fragmentation if DP is set too high. The entrance potential (10 kV) was kept at this default value. The new DP value was entered in the software before doing a product ion scan to roughly determine the two most abundant unique fragments while changing the collision energy (CE). Finally, MRM was used to optimize the CE and collision exit potential (CXP) for a specific transition. Table 2-2 summarizes the final MRM method. Other optimized MS parameters are as follows: collision activated dissociation (CAD) gas: 4; curtain gas (CUR): 10; nebulizer gas (GS1) and auxiliary gas (GS2): disabled (not applicable with the interface); IS: 4500 V; resolution of Q1 and Q3: unit.

Table 2-2: List of MRM channels and parameters used for the metabolites and their internal standards.

Analyte	Q1 Mass	Q3 Mass	DP (V)	CE (V)	CXP (V)	Dwell time (ms)
Sarcosine	90	44	40	19	3	30
L-Pro	116	70	35	20	10	30
L-CysCys (dimer)	241.2	152.2	35	19	10	30
L-Leu	132.1	43	40	37	8	30
L-Glu	148.1	84.1	45	21	7	30
L-Kyn	209.2	94.1	55	19	7	30
*Sarcosine-D ₃	93	47	40	19	3	30
*L-Methionine sulfone	182.1	136.2	60	15	10	30

Cysteine readily oxidizes in air to produce a dimer known as cystine. $[M+H]^+$ of cysteine ($m/z = 122$) was barely detectable in the full scan mode, but the dimer ($m/z = 241$) was observed and used to quantify cysteine.

2.3 RESULTS AND DISCUSSION

2.3.1 Sarcosine

- *Separation from its isomers*

The main objective of our study was to provide a practical screening method for sarcosine and other potential PCa biomarkers. It is probably not widely known that sarcosine has two other isomers, namely α - and β -Ala. An LC/MS technique typically takes the derivatization route to separate these three compounds. Though underivatized LC/MS separation has been attempted by Jiang *et al.*⁵¹, they were unable to distinguish between sarcosine and α -Ala since they have identical transition channels (m/z 90 > 44).

Separation and identification of sarcosine from its isomers is crucial for quantitative analysis as the small quantity of sarcosine is often obscured by the larger peaks of its isomers in biological samples. The total ion electropherogram and extracted ion electropherograms

of native urine sample are shown in Figure 2.4a. The standards (Figure 2.4b) show clearly that β -Ala has a unique transition (m/z 90 > 72) in addition to well-resolved electrophoretic separation from sarcosine and α -Ala. On the other hand, the most sensitive transition for sarcosine is identical to α -Ala, giving the same m/z fragments. Since endogenous level of α -Ala in urine is much higher than that of sarcosine's, the two must be electrophoretically separated for quantitative purposes. The periodic noise in Figure 2.4b was caused by a very small bubble at the sprayer outlet. Because there was no intention of using the data for quantification, we did not repeat this experiment after the bubble was flushed away in subsequent experiments. As can be seen in Figure 2.4a and the rest of electropherograms in this chapter, the baseline was very stable.

The migration order of the three isomers is explained by the fraction of protonated species at the pH of the buffer used (~ 2.50) during separation.

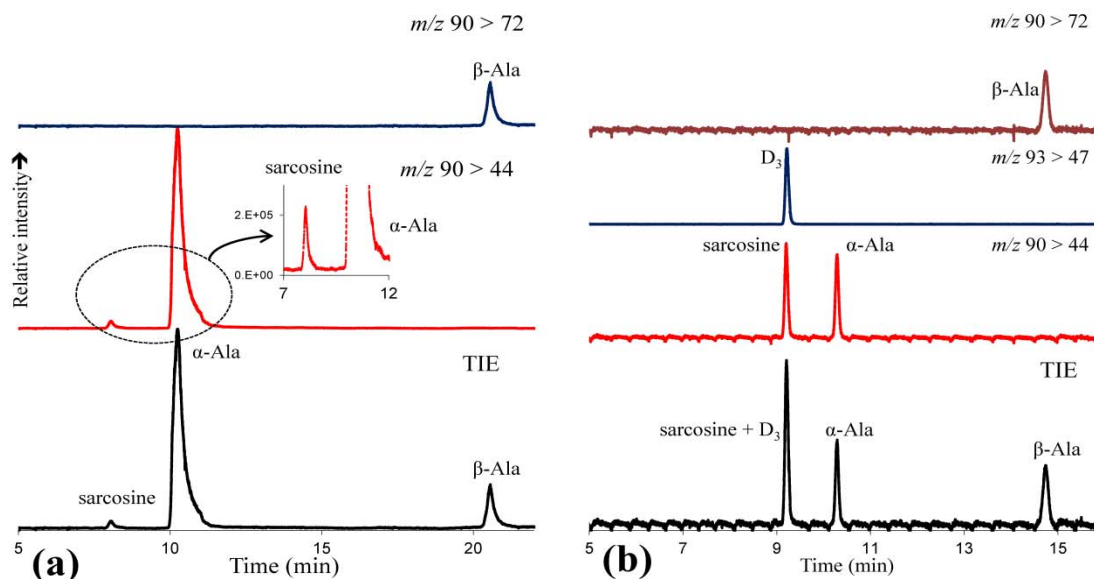


Figure 2.4: Representative total ion electropherograms (TIEs) and extracted ion electropherograms of (a) native urine and (b) 0.01 mM standard mix. BGE and modifier, 0.4% formic acid, 50% methanol; modifier flow rate, 200 nL min⁻¹; sample in buffer injected at 0.5 psi for 5 s; CE inlet, -30 kV; Needle, 4.5 kV; MS/MS conditions, in Table 2-2 and Section 2.2.5.

- *SPE recovery*

To achieve maximum SPE efficiency, we studied different variables outlined in the flow chart shown in Figure 2.2. A significant part of our method development was spent on sensitivity enhancement in detecting endogenous sarcosine in urine. This depends not only on the sensitivity of the MS instrument available to us but also on the efficiency of the extraction procedure. For this reason, the LCQ ion trap MS was used for optimizing separation conditions (e.g., buffer selection) as it was incapable of detecting endogenous sarcosine due to its poor sensitivity. The final method was eventually transferred into the more sensitive triple quadrupole MS for MRM analysis.

In order to calculate the recovery or efficiency of an extraction procedure, a blank matrix, a urine sample that does not contain the analyte of interest, is necessary. Because sarcosine is endogenous in urine, some laboratories choose simulated or synthetic urine. However, we decided to use real samples and deuterated sarcosine to estimate the recovery of sarcosine. Deuterated sarcosine (methyl-D₃) and a second IS (L-methionine sulfone) were spiked into the pooled urine, and calculations were based on the ratio of the areas of extracted and non-extracted D₃ over the area of L-methionine sulfone. The recovery of the optimized SPE procedure was found to be $94.4 \pm 7.4\%$ ($n = 3$).

- *Precision, accuracy and linearity*

Intra-day precision and accuracy were evaluated by analyzing five individually extracted samples of six different concentrations on the same day. The peak area ratio of sarcosine to D₃ was plotted against the added concentration of sarcosine. The endogenous level of sarcosine was determined from the x -intercept of the calibration curve. Concentration of the original 100 μ L aliquot was calculated by multiplying the x -intercept to the pre-concentration factor of 5. Conversely, inter-day precision and accuracy were determined by analyzing three individually extracted samples of each concentration for three consecutive days. Inter-day results were calculated using the same calibration curve from intra-day calibration. Precision and accuracy values for intra-day and inter-day are presented in Table 2-3. Variations in inter-and intra-day measurements are all less than 15% which conform to the International Guideline for *Bioanalytical Method Validation*⁶⁶. Similarly, accuracy values are within 15% of the added concentration except for the lowest standard, 0.50 μ M, found at 80% and 124% for intra-day and inter-day, respectively. The anomaly is explained by the calibration starting to deviate from linearity below 0.50 μ M. The deviation

is not a serious concern to the overall method for two reasons: first, the endogenous concentration of sarcosine in the pre-concentrated extracted urine is $4.93 \pm 0.19 \mu\text{M}$ which is greater by one order of magnitude than the lower limit of quantitation, $0.50 \mu\text{M}$; second, according to Sreekumar et al.³⁴, sarcosine concentration in urine was found to increase significantly during prostate cancer progression. Therefore, the limit of detection and calibration for sarcosine are adequate for concentrations expected in a clinical study.

Table 2-3: Inter-day (n = 5) and intra-day (n = 3) precision and accuracy of peak area ratio and recovery of sarcosine by CE–ESI-MS/MS.

Added concentration (uM)	Peak area ratio (RSD %)		Intra-day			Inter-day		
	Intra-day	Inter-day	Found (μM)	Accuracy (%)	RSD %	Found (μM)	Accuracy (%)	RSD %
0.00	3.58	7.00	--	--	--	--	--	--
0.50	0.43	0.93	0.40	80	5.85	0.62	124	8.43
1.00	1.92	1.63	0.91	91	12.5	0.96	96	10.1
2.50	4.78	--	2.51	100	14.3	--	--	--
5.00	4.73	5.23	5.82	116	8.78	5.26	105	10.2
10.0	3.69	4.39	10.5	105	5.44	10.1	101	6.56
20.0	1.60	--	19.5	98	2.01	--	--	--

Linearity of the method was assessed by spiking pooled urine with 0–20 μM sarcosine standards, spanning the range of 0.1–4 times the estimated endogenous concentration. The intra-day and inter-day calibration curves have good linear fits with $R^2 = 0.9951$ and 0.9990 respectively (Table 2-4). The creatinine normalized concentration of sarcosine in pooled urine in the original 100 μL sample was found to be $0.10 \pm 0.01 \mu\text{mol/mmol}$ of creatinine which is in agreement with the normal range reported by the *Human Metabolome Database*⁶⁷⁻⁶⁹.

Table 2-4: Summary of results for inter-day (n = 5) and intra-day (n = 3) calibration of sarcosine in pooled urine.

Validation Parameters			
Regression equation ^a		Linear	
Intra-day	$y = (1.72\text{E-}02 \pm 2.73\text{E-}04)x + (8.59\text{E-}02 \pm 2.23\text{E-}03)$		$R^2 = 0.9951$
Inter-day	$y = 1.81\text{E-}02x + 8.19\text{E-}02$		$R^2 = 0.9990$
Limit of detection (μM)	0.0176		
Linear range (μM)	0.50 - 20.0		
SPE efficiency (n=3)	94.4 ± 7.4%		
Endogenous sarcosine concentration in 100 μL urine sample prior SPE(μM)	0.99 ± 0.04 ^b	or	0.10 ± 0.01 μmol/mmol of creatinine <0.329; 0.476 ^c μmol/mmol of creatinine

^a y and x stand for peak area ratio (sarcosine/IS) and concentration in μM respectively.

^b Endogenous concentration calculated from the x -intercept of the intra-day standard addition graph; standard deviation of x -intercept calculated by $SD = s_y / |m| \sqrt{(1/n + \bar{y}^2 / m^2 \sum (x_i - \bar{x})^2)}$, where m is the slope; n is the # of data points; \bar{y} is the mean value of y ; \bar{x} is the mean value of x ; and s_y is the standard deviation of y .

^c Normal range for healthy adults (>18 years) based on literature ⁶⁷⁻⁶⁹.

2.3.2 Other metabolites

- *Sample preparation*

L-Pro, L-Cys, L-Leu, L-Glu, and L-Kyn were all found to saturate the MS detector after SPE. The SPE procedure has a preconcentration factor of 5: from the initial sample volume of 100 μL, to a final reconstitution volume of 20 μL. The sample was then further diluted by 20-fold. The estimated endogenous concentrations of L-pro, L-Cys, L-Leu, L-Glu, and L-Kyn in urine are ~38, ~416, ~107, ~331, and ~11 μM respectively. This estimation was necessary to roughly determine the amount of each analyte in urine, thus allowing the selection of relevant concentration range for the validation process. The estimation was done by a single-point calibration using a blank and a spiked urine sample. At this point, we realized that it may not be necessary to extract and preconcentrate the analytes as they are already present in very high concentrations in native urine. Although we were initially concerned about possible matrix effects when bypassing SPE, we realized that urine has a

less complex matrix compared to other biological samples such as plasma and tissue. In addition, the rinsing and conditioning procedure between runs developed for this work is capable of eliminating the adverse effect from analyzing these samples. With this rationale, we omitted SPE and filtered the urine samples using 5 kDa molecular cutoff cellulosed based filters before further diluting 15-fold in buffer. Using similar single-point calibration, we roughly estimated the endogenous levels of L-Pro, L-Cys, L-Leu, L-Glu, and L-Kyn to be approximately ~48, ~533, ~186, ~256, and ~11 μM , respectively. These values seem to agree with the previous estimated concentrations, although the majority of them are higher. However, since they were only estimated from a single-point calibration, they are not as accurate as the endogenous concentrations determined by a full validation summarized in Table 2-5 and 2-6. The concentrations in Table 5 are the final concentrations of the analytes after dilution. We are confident that the recovery and accuracy obtained using this method are greater than otherwise acquired using SPE, since they did not undergo extraction and were analyzed directly.

Table 2-5: Intra-day precisions (n = 3) and accuracies of five metabolites by standard addition method of diluted urine. Final concentrations are calculated based on dilutions made during sample preparation.

L-Pro			L-CysCys			L-Leu			L-Glu			L-Kyn		
Concentration (μM)	Accuracy (%)	RSD %	Concentration (μM)	Accuracy (%)	RSD %	Concentration (μM)	Accuracy (%)	RSD %	Concentration (μM)	Accuracy (%)	RSD %	Concentration (μM)	Accuracy (%)	RSD %
0.57	90	5.72	2.84	111	3.54	2.27	104	5.10	2.84	92	12.4	0.11	112	13.4
1.14	103	5.31	5.68	115	14.0	4.55	103	3.71	5.68	104	1.50	0.23	98	7.65
2.27	103	1.91	11.4	100	2.32	9.1	101	0.92	11.4	100	0.66	0.45	98	3.47
4.55	103	1.50	22.7	101	1.85	18.2	101	2.20	22.7	101	4.61	0.91	103	1.79
9.10	100	0.27	45.5	95	0.15	36.4	98	0.03	45.5	100	0.29	1.82	100	0.56
18.2	100	0.10	91.0	101	0.39	72.8	100	0.32	91.0	100	0.52	3.64	100	0.52

Table 2-6: Summary of intra-day (n = 3) results for non-SPE sample validation.

	Calibration curve	R ²	LOD (μM)	Concentration of pooled urine ± SD (μmol/mmol of creatinine) ^{a,b}	Literature value (μmol/mmol of creatinine) ^c	Linear range (μM) ^d
L-Pro	$y = (1.67 \pm 0.01)x + (0.790 \pm 0.045)$	0.9998	0.134	0.74 ± 0.06	0.86	0.63 - 20.0
L-CysCys	$y = (0.098 \pm 0.001)x + (0.448 \pm 0.030)$	0.9989	0.034	7.12 ± 0.69	10.5	3.13 - 100
L-Leu	$y = (0.125 \pm 0.001)x + (0.233 \pm 0.012)$	0.9998	0.131	2.91 ± 0.24	3.57	2.50 - 80.0
L-Glu	$y = (0.478 \pm 0.002)x + (0.813 \pm 0.064)$	0.9998	0.116	2.66 ± 0.28	1.39	3.13 - 100
L-Kyn	$y = (0.492 \pm 0.002)x + (0.070 \pm 0.003)$	0.9997	0.010	0.22 ± 0.02	0.41	0.13 - 4.00

^a Endogenous concentration calculated from the x -intercept of the standard addition graph; standard deviation of x -intercept calculated by

$$SD = s_y / |m| \sqrt{1/n + (y^2/m^2 \sum (x_i - \bar{x})^2)}$$

^b Standard deviations (SDs) calculated using relative uncertainties of x -intercepts and creatinine concentration.

^c Values obtained from Refs. ⁶⁷⁻⁶⁹.

^d Reported linear range corresponds to concentration of added standards before dilution without taking into account the endogenous metabolite concentrations.

- *CE-MS/MS analysis*

The only drawback we found for eliminating SPE was that we had to perform additional rinsing steps in the CE procedure to ensure reproducibility of migration times. The PEI coated capillary provided fast analysis times (~15 min), as depicted in Figure 2.5, without the need for pressure assistance. The analytes were not completely resolved in the total ion electropherograms (TIEs), but individual MRM channels were checked for “cross talk” between analytes. Complete separation and identification of all peaks were carried out for channels that contain more than one peak such as L-Leu. The more sensitive but common transition (m/z 132 > 86) was not used for L-Leu to minimize isobaric interferences from isoleucine and *allo*-isoleucine. Other isobars, 4-hydroxy-L-proline and ϵ -aminocaproic acid, were fully resolved from L-Leu in the channel of m/z 132 > 43, which was used in this method.

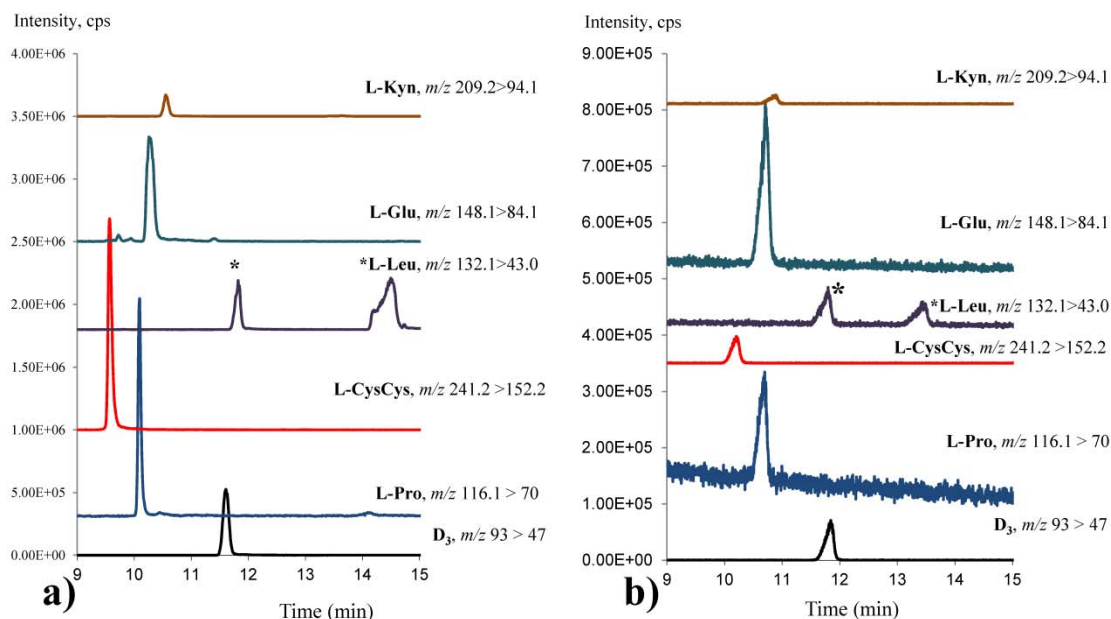


Figure 2.5. Extracted ion electropherograms of (a) 100-μL SPE native urine sample and (b) Non-SPE 15-fold diluted native urine sample. BGE and modifier, 2.0% formic acid, 50 % methanol; modifier flow rate, 200 nL min⁻¹; sample in buffer injected at 1 psi for 10 s; CE inlet, -30 kV; Needle, 4.5 kV; MS/MS conditions, in Table 2-2 and Section 2.2.5.

The PEI coating minimizes adsorption of positively charged peptides and proteins to the capillary wall. Yet we discovered that with a buffer rinse alone, the migration times were delayed considerably after each diluted urine sample was analyzed. Various combinations of rinsing solvents/solutions were examined. The sequence that gives the most reproducible results is methanol, air, and buffer rinses. This series of rinses must be performed between each analysis of non-SPE diluted samples to condition the coating and flush unwanted molecules that are adsorbed to the capillary walls.

- *Method validation: precision and accuracy*

A standard addition method was employed for calibrating the five metabolites in diluted urine sample. Endogenous amounts of each analyte were roughly estimated first and the value of calibration standards were adjusted so that the endogenous concentrations are in the range of the chosen standards. A summary of results is shown in Table 2-5, which demonstrates excellent precision and accuracy values in all cases. Accuracy values range from 90 to 112%, while precision variations are <13.38% in which the greatest variation and lowest accuracy occurs for the least concentrated standard for each analyte.

- *LOD, LLOQ, and linear range*

LOD values reported in Tables 2-4 and 2-6 were calculated based on the concentration that will give a peak height of three times the noise level ($S/N = 3$). S/N calculation is based on an algorithm in the *Analyst*® software where the adjacent region of the peak is defined as the noise level. The dynamic range was tested on neat aqueous solutions and urine samples. The calibration demonstrates good linearity for all metabolites over the validation standards. The lower limit of quantitation (LLOQ), defined as the lowest concentration that is within $\pm 20\%$ RSD, is most likely to be lower than the least concentrated standard for each analyte as indicated by their respective RSD values (< 15%).

The endogenous concentration of each analyte was calculated from the calibration curve. They were then normalized over creatinine concentration as it is the standard practice when expressing metabolite concentrations in urine. Our experimental endogenous concentrations agree with existing values obtained from the *Human Metabolome Project* database⁶⁷⁻⁶⁹.

2.3.3 Stability

Bench-top stability of SPE processed samples was determined by analyzing a sarcosine-D₃ spiked urine blank over the course of 1h, 12 h, and 24 h at room temperature. Sarcosine was found to be stable for 12 h at room temperature with little variation in the peak area ratio. The degradation of sarcosine within the first 12 h was not significant. However, after 24 h at room temperature, the signal and calculated concentration decreased by 25%. For freeze–thaw stability, sarcosine was found to be stable over three FT cycles (<7% RSD).

Stability of non-SPE diluted samples was assessed differently because they did not go through SPE. Therefore, they have to be tested under more rigorous conditions. Freshly diluted spiked urine samples were analyzed within 2 h and kept in the refrigerator at 4 °C for 7 days and analyzed again. No significant variation (<10% RSD) on the peak area ratios of L-Pro, L-Cys, L-Leu, L-Glu, and L-Kyn were found after 7 days in the refrigerator.

2.4 CONCLUSIONS

We have developed a method for quantifying low level analytes such as sarcosine in urine without derivatization. Excellent resolution was achieved between sarcosine and its isomers, α - and β -Ala, even with the use of a positively charged PEI-coated capillary with a very fast electroosmotic flow (EOF). The optimized SPE protocol and preconcentration technique yielded very good recovery for sarcosine ($94.4 \pm 7.4\%$). On the other hand, an extraction procedure was not necessary for analyzing high concentration urinary metabolites, and the sample must be diluted to avoid MS detector saturation. Separate calibrations for low and high level analytes could indeed become laborious particularly for clinical study applications. Perhaps a more sensitive MS would allow us to detect sarcosine from diluted

non-SPE samples. Regardless of the circumstances, we are confident that the method developed is validated for potential PCa biomarker screening and we look forward to embarking on our own clinical study and finding an answer to the intriguing question of whether sarcosine and other metabolites are indeed potential biomarkers.

Chapter 3: Towards chiral separations by capillary electrophoresis mass spectrometry using cyclodextrins as chiral selectors

3.1 INTRODUCTION

According to the theory of chiral recognition, a minimum of three simultaneous interactions, also known as the “three-point rule”, for one of the enantiomers is required and at least one of them must be stereoselective⁷⁰. These three interactions are generally a combination of attractive and repulsive forces, such as formation of hydrogen bonds, ionic interactions, hydrophobic interactions, and host-guest complexations. The three-point model has been widely applied in chromatography for the development of commercial chiral stationary phase (CSP) columns for enantiomeric separations. Many of these CSP columns are composed of oligosaccharide molecules, in particular cyclodextrins (CDs) and their derivatives.

Cyclodextrins are cyclic oligomers made of 5 or more D-glucopyranoside molecules. They are classified based on the number of glucose units they possess. For example, the three naturally occurring cyclodextrins in Figure 3.1: namely, α -CD, β -CD, and γ -CD have 6, 7, and 8 glucopyranoside units, respectively. As the number of hydroxyl groups increases, their solubility in water increases. However, due to internal hydrogen bonding between its secondary hydroxyl groups, β -CD is an exception to this rule. It has a lower solubility than α -CD. To increase the overall solubility of CDs in water, modifications are possible by introducing functional groups at the 2nd, 3rd, and 6th hydroxyl positions.

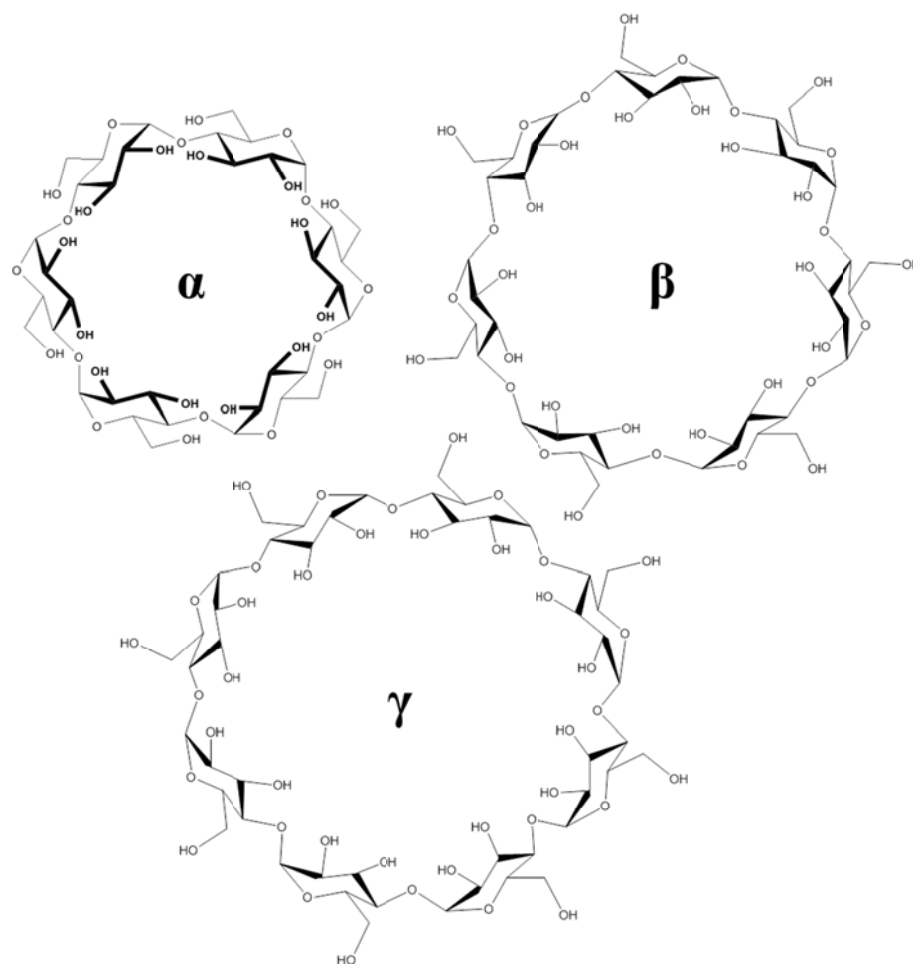


Figure 3.1: Structures of naturally occurring cyclodextrins: α -CD, β -CD, and γ -CD.

Cyclodextrins possess a truncated cone structure in which the hydroxyl groups are oriented toward outside, giving them a hydrophilic exterior and a hydrophobic interior cavity. They can make inclusion complexes with a variety of compounds. With each glucose unit containing five chiral centres, this host-guest interaction satisfies the steric requirements for enantiomeric separation⁷¹. As a general rule, the cavity dimension of α -CD is appropriate for monocyclic aromatic hydrocarbons; β -CD is suitable for molecules containing naphthalene rings; and γ -CD with three aromatic rings.

A group of derivatized charged CDs have gained tremendous popularity in chiral CE during the last decade⁷²⁻⁷⁴. In contrast to neutral CDs, highly-sulfated cyclodextrins (HS-CDs) are modified CDs that exist as anions even at very low pH buffers. As a result, they have been widely used in chiral and achiral separations of numerous compounds including neutral analytes. Their unique mechanism of action is depicted in the diagram below (Figure 3.2). At very low pH, EOF is negligible on uncoated capillaries. Positively-charged analytes will migrate toward the cathode under normal polarity. Conversely, anionic CDs will move toward the opposite direction. Theoretically, this amplifies chiral recognition because analytes experience a longer separation window “as the maximum opportunity for separation exists when the analyte and anionic CD migrate in opposite directions⁷²”.

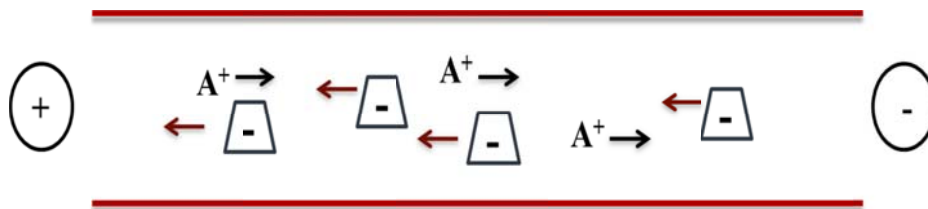


Figure 3.2: The countermigration mechanism of anionic highly-sulfated CDs. A⁺: analytes; vessels: HS-CDs.

The net electrophoretic mobility (μ_{ep}^A) of an analyte in a single additive system can be expressed as the sum of the electrophoretic mobility of the free analyte, ($\mu_{ep,A}$), and the complexed analyte, ($\mu_{ep,AC}$)⁷⁵:

$$\mu_{ep}^A = f\mu_{ep,A} + (1 - f)\mu_{ep,AC} \quad (3-1)$$

where f is the fraction of the free analyte: $[A]/([A] + [AC])$. Eqn. 3-1 can also be rewritten in terms of the equilibrium constant, K , and the concentration of the chiral selector, $[C]$:

$$A + C \rightleftharpoons AC \quad K = \frac{[AC]}{[A][C]} \quad (3-2)$$

$$\mu_{ep}^A = \frac{\mu_{ep,A} + K[C]\mu_{ep,AC}}{1 + K[C]} \quad (3-3)$$

Since the two enantiomers will have identical $\mu_{ep,A}$, the separation between enantiomers is dependent on the $\mu_{ep,AC}$, K , and $[C]$.

Instead of switching CSP packed columns in chromatography, selectivity of a particular separation in CE is manipulated by adjusting simple parameters. A group of racemic amino acids were chosen for this study to demonstrate the ease in using CDs as BGE additives in CE. CDs and their derivatives have widespread applications in CE, especially in pharmaceutical⁷⁶, clinical⁷⁷, and food analysis⁷⁸. In addition, cyclodextrins do not significantly absorb in the UV/vis range wavelength which make it an attractive choice of detection both in chromatography and electrophoresis. More recently, however, the online coupling of CE to MS through the use of ESI interfaces has significantly enhanced the sensitivity and selectivity of CE separations⁷⁹. MS provides the power of obtaining structural identification of unknown chiral compounds in complex matrices and real samples. Although CE is a very successful enantiomeric separation technique, there are specific challenges involved with transferring methods developed for CE-UV to CE-ESI-MS. Some of these issues include: the use of volatile buffers; the current mismatch between CE and ESI; and most importantly, the ion suppression effect and ion source contamination caused by using non-volatile chiral selectors such as CDs.

This chapter presents the work in developing a chiral CE-UV method, while keeping in mind the requirements for a successful transfer to CE-ESI-MS analysis.

3.2 EXPERIMENTAL

3.2.1 Chemicals and solutions

L- and D-Tryptophan (Trp), L- and D-tyrosine (Tyr), DL-3,4-dihydroxyphenylalanine (DL-DOPA), and DL- kynurenine (Kyn) with minimum of 98% purity were purchased from Sigma Chemical Co. (St. Louis, MO). α -Cyclodextrin (α -CD), sodium phosphate monobasic ($\text{NaH}_2\text{PO}_4 \cdot \text{H}_2\text{O}$, 99.0%), formic acid (88%), NaOH, HCl, methanol (HPLC grade), and glacial acetic acid were purchased from Fisher Scientific (Nepean, ON, Canada). Highly sulfated (HS)- α -, β -, and γ - cyclodextrins with stock concentrations of 20% (w/v) were kindly donated by Beckman Coulter (Brea, CA, USA). PEI coating reagent of trimethoxysilylpropyl-modified polyethylenimine, 50% in isopropanol was purchased from Gelest Inc. (Morrisville, PA).

Buffers and analyte stock solutions were weighed within ± 0.0010 g accuracy. Stock solutions (10 mM) of L-Trp, D-Trp, L-Tyr, D-Tyr, and DL-Kyn were prepared by dissolving the appropriate amount in 18 M Ω water acidified with 0.1 M HCl. Due to its short half-life, DL-DOPA was prepared freshly every 2 weeks and stored in an amber glass bottle at -20°C . Buffers were sonicated and then adjusted to the required pH by adding 1.0 M NaOH, 6 M or 3 M HCl, dropwise, monitored by a Beckman Φ 340 pH/temperature meter within ± 0.05 pH unit to the desired pH. All other reagents were of analytical grade and every solution was filtered through 0.22- μm , sterile Nylon syringe filters and stored at 4°C in a refrigerator.

3.2.2 Instrumentation and electrophoretic procedure

A Beckman P/ACE™ System MDQ Capillary Electrophoresis unit (Brea, CA, USA) equipped with photodiode array (PDA) detector was employed for all CE analysis. Experiments were carried out on varying lengths of fused silica capillary, bare or coated with cationic PEI, and both having dimensions of 50- μ m ID \times 365- μ m OD (Polymicro Technologies, Phoenix, AZ). Analytes were detected at either 200 or 214 nm using direct absorbance. Normal and reverse polarity were used for experiments carried out on uncoated capillary while reverse polarity was used for the PEI coated capillary. The capillary temperature was maintained at 22 °C using the temperature controlled coolant system of the CE.

New uncoated capillaries were conditioned prior to use by rinsing at 30 psi with methanol for 5 min, followed by deionized water for 5 min, 1 M NaOH for 15 min, deionized water for 3 min, and finally with BGE for 15 min. At the beginning of each day before starting any experimental runs, the capillary was rinsed at 30 psi with 0.1 M NaOH for 15 min and corresponding BGE for 15 min. Before each injection, the capillary was rinsed at 30 psi for 5 min with 0.1 M NaOH, 2 min with deionized water, and finally 5 min with the run buffer. Samples were injected into a BGE filled capillary at 0.5 psi for 4 s.

For every CE run in coated capillaries, before each injection, the separation capillary was rinsed with buffer for 3 min at 40 psi. When the migration time of the analytes were observed to slow down, the coated capillary was conditioned by flushing it with methanol at 40 psi (5 min), air at 40 psi (5 min), deionized water at 40 psi (5 min), and finally the BGE

at 40 psi for 15 min. When the coated capillary was not in use, it was filled with deionized water and the tips were immersed in water to prevent it from drying out.

3.3 RESULTS AND DISCUSSION

3.3.1 Separation performance of coated and uncoated capillaries

D- and L-Trp have been separated with uncoated fused silica capillary under normal polarity and in a coated capillary under reverse polarity, using the following experimental conditions: capillary length (L_t), 50 cm; BGE, 50 mM α -CD in a 100 mM (pH 2.5) sodium phosphate buffer. α -CD was chosen among the three natural CDs as the more suitable CS for tryptophan and this decision was supported by studies in literature^{80, 81}. Since the isoelectric point (pI) of tryptophan is 5.89, a low pH buffer (pH = 2.5) was selected to maximize the probability of protonated states of the analyte. Positive ion mode is more sensitive in most of the mass spectrometers. For uncoated fused silica capillaries, the rate of EOF is very much dependent on the pH of the buffer. At pH < 3, the magnitude of EOF is very low as a consequence of the non-ionized silanol groups on the capillary wall. The charge state of α -CD is neutral and the electrophoretic mobility of its native form is zero. In contrast, the positively-charged PEI-coated capillary generates fast anodic EOF when a buffer with low pH is used. Therefore, the polarity is reversed in order to detect the analytes. A resolution (R_s) of 4.45 between D- and L-Trp was achieved in an uncoated capillary, two times greater than that obtained in the PEI-coated capillary ($R_s = 2.04$). However, the analysis time (7 min) and efficiency ($N \sim 127000$) were significantly better in the PEI-coated capillary compared to the values obtained in uncoated capillary ($t_m = 24$ min; $N \sim 40500$). A compromise between resolution, analysis time, and peak efficiency is vital especially in

practical applications. In addition to very short analysis times and extremely sharp peaks, the resolution achieved for D- and L-Trp in the PEI-coated capillary was more than sufficient for qualitative or quantitative purposes. For this reason, subsequent chiral investigations on α -CD were all performed with a coated capillary. The choice of buffer also needed to be addressed at this point since the current generated with 100 mM sodium phosphate BGE on a PEI-coated capillary was too high ($\sim 80 \mu\text{A}$) for CE/MS analysis. Buffers that contain salts, phosphates, sulphates, and detergents should be avoided for MS. Their presence not only generates high currents, but also suppresses the ion signal and contaminates the ion source. Therefore, a volatile buffer composed of formic acid was used instead of phosphate to alleviate these problems. At 0.18% formic acid, the pH of the separation buffer was maintained at ~ 2.5 .

3.3.2 Effect of CD concentration on resolution

The effect of α -CD concentration on the resolution was studied by varying its concentration from 0 to 50 mM while keeping all the other parameters constant. The resolution between D- and L-Trp was calculated for each concentration and the results are shown in Figure 3.3. Below 20 mM α -CD, no separation was observed between the enantiomers, but when the concentration was increased from 20 to 50 mM, L-Trp and D-Trp began to separate. Resolution improved at higher α -CD concentrations due to a higher number of complexes formed between the neutral CDs and the analytes. The electrophoretic mobility of the analytes is inversely proportional to the viscosity of the buffer solution, hence at higher CD concentrations, the migration times of the analytes were increased. The current generated was reduced to 3 – 4 μA in all α -CD concentrations using formic acid buffer at a separation voltage of -10 kV in a 60-cm long capillary. Despite the smaller field strength

produced by lower applied voltage and longer capillary, the analysis time for the coated capillary was still within 15 min. However, in terms of separation efficiency and peak shape, the phosphate buffer is still superior to formic acid. At the same 50 mM α -CD concentration, the resolution achieved in phosphate buffer ($R_s = 2.04$) was reduced to half using formic acid buffer ($R_s = 1.18$).

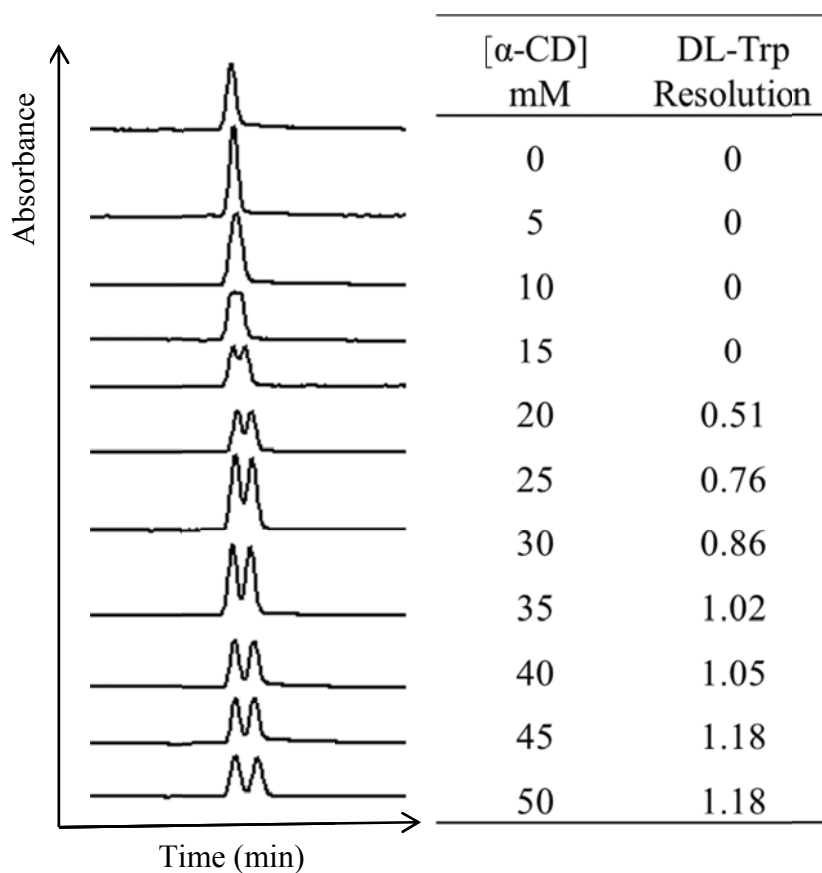


Figure 3.3: Effect of α -CD concentration on the resolution of DL-Trp on a PEI coated capillary. CE conditions: L_T , 60 cm; BGE, 0.18% formic acid, (pH 2.5); -10 kV; capillary temperature, 22°C ; wavelength detection, 214 nm.

3.3.3 Effects of voltage and capillary length on resolution

The resolution between two adjacent peaks is described by the equation:

$$R_s = \frac{t_{m2} - t_{m1}}{2(w_1 + w_2)} \quad (3-1)$$

in which t_m and w are the migration times and corresponding peak widths of the two enantiomers, respectively. The effect of voltage on resolution is not simple. It is actually influenced by several factors such as Joule heating, EOF, and the electrophoretic mobilities of the analytes. In the case of DL-Trp, a maximum resolution was observed at 15 kV (Figure 3.4). As the magnitude of the applied voltage was lowered from 22.5 kV to 15 kV, the migration times of the analytes increased. The electrophoretic mobilities of the analyte and EOF will decrease accordingly, prolonging the interactions between the CS and the analyte. The decline of R_s as the voltage rose from –15 to –22.5 kV could be attributed to reduction of separation efficiency due to Joule heating. On the other hand, when the voltage was further lowered from –15 kV to –5 kV, the resolution began to decrease again as a result of band broadening at lower migration rates, in this case caused by diffusion.

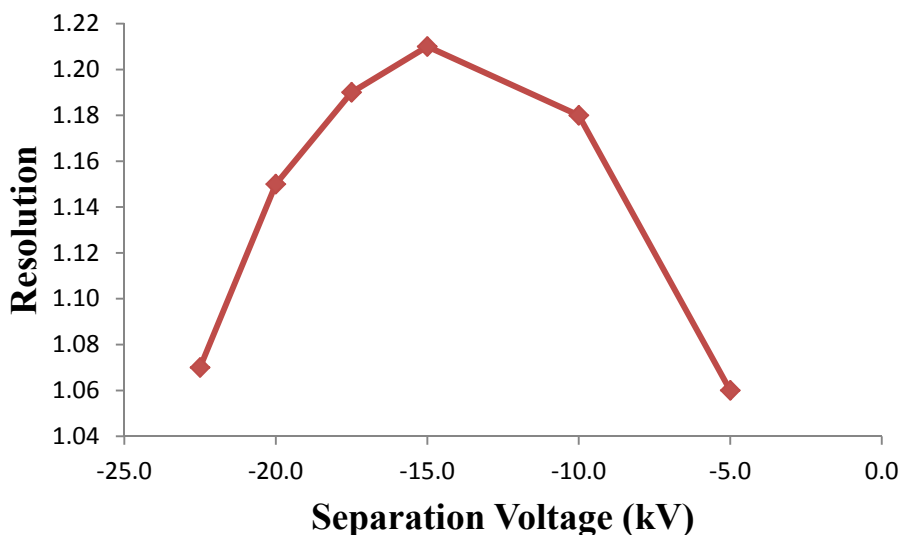


Figure 3.4: Effect of applied voltage on R_s of DL-Trp on a PEI coated capillary. CE conditions: LT, 60 cm; BGE, 0.18% formic acid, (pH 2.5); capillary temperature, 22 °C; wavelength detection, 214 nm.

Longer capillaries result in smaller field strengths when the same voltage is applied, hence longer migration times. Although the effect of diffusion can still reduce resolution, in this particular study, the relationship between capillary length and R_s is more obvious. The resolution was clearly improved as the total length of the capillary was increased. Under the same experimental conditions and choosing 15 kV as the optimum voltage, the resolutions obtained for 48 cm, 60 cm, and 95 cm, were 0.45, 1.15, and 1.72, respectively. There is also a limit, of course, in the length of the capillary because when the length is too long, the reduced field strength and the longer migration time will lead to additional band broadening.

3.3.4 Effect of organic modifier: methanol

Addition of organic modifiers in BGE can alter the inclusion selectivity, EOF, stability of the inclusion complexes, solubility of the CDs, and conductivity and pH of the BGE. The presence of organic solvent such as DMSO, DMF, acetonitrile, alcohols and other dipolar solvents can lead to a dramatic enhancement or reduction in resolution. As mentioned previously in the first chapter, addition of organic modifier in the BGE is also essential to help the desolvation of the analyte ions during the ionization process in MS. Since our ultimate goal is to successfully transfer this CE–UV method to CE–ESI–MS, we must work towards using the conditions required for MS through every step in our method development.

Methanol has been an indispensable component in the BGE and modifier solutions from our biomarkers CE–ESI–MS work in Chapter 2. The percentage of methanol (v/v) in the buffer was varied from 1% to 20% and the electropherograms obtained are presented in

Figure 3.5. Unfortunately, addition of methanol in the BGE was quite detrimental to the resolution of D- and L-Trp. Figure 3.5 shows that at 2.5% methanol, the resolution between the enantiomers has completely vanished. This is likely due to the limited solubility of α -CD in methanol-water mixtures⁸².

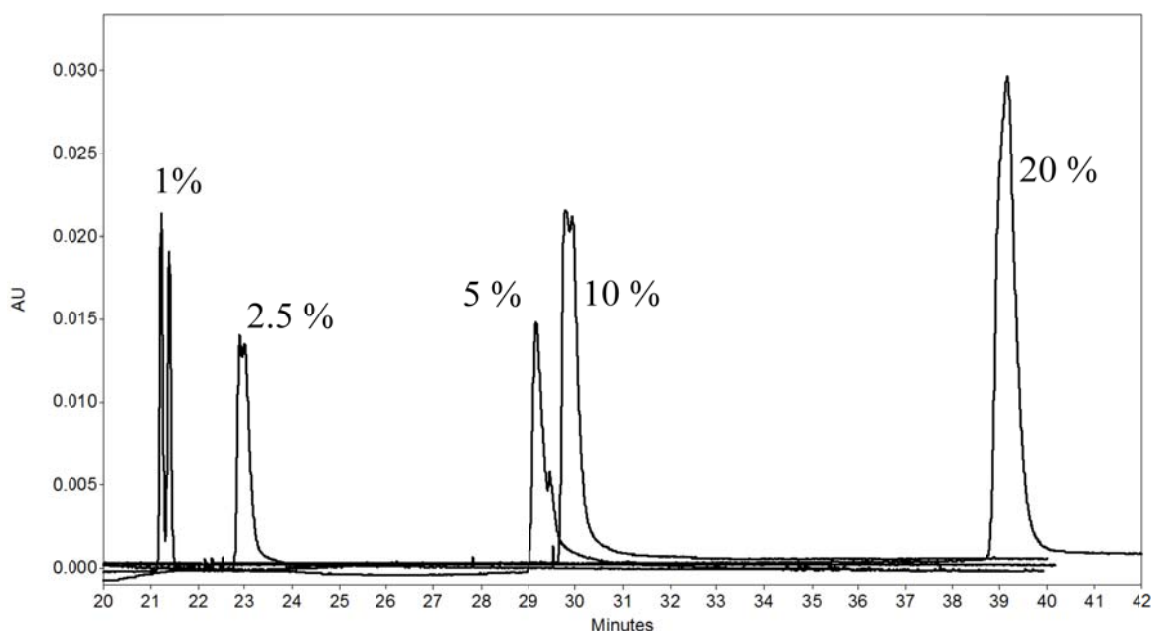


Figure 3.5: Effect of adding methanol in BGE on resolution of DL-Trp. CE conditions: L_T , 95 cm; BGE, 0.18% formic acid, (pH 2.5); capillary temperature, 22 °C; wavelength detection, 214 nm; voltage, -10kV.

Other organic solvents such as acetonitrile and isopropanol should also be investigated. Nevertheless, it is not entirely necessary for the separation buffer to contain an organic solvent. The CE-ESI-MS interface developed in our group allows the use of higher volatile content in the chemical modifier solution to compensate for its absence in BGE and thus help the desolvation and ionization processes. Hence, instead of investigating other organic modifiers, the last part of this chapter focuses on a group of charged CD derivatives

as an attractive alternative to neutral CDs for chiral CE separation in MS amenable conditions.

3.3.5 Derivatized CDs: highly-sulfated cyclodextrins

In addition to DL-Trp, DL-Tyr, DL-DOPA, and DL-Kyn were added to the sample mixture to investigate the feasibility of HS-CDs in chiral resolution. At pH 2.5, EOF is generally suppressed on uncoated capillaries, but the charge state of HS- α -CD, HS- β -CD, and HS- γ -CD will still be negative. Figure 3.6 shows the separation of these four pairs of enantiomers under normal polarity using 5% of each HS-CD on a bare-fused silica capillary. Excellent separation between each enantiomer was obtained at 5% HS- β -CD and HS- γ -CD in the BGE. However, at these experimental conditions, the current generated was between 90 to 120 μ A which was obviously incompatible to the ESI current. The high current generated is a consequence of the charged HS-CDs; thus, in order to decrease its magnitude, lower HS-CD concentrations were employed.

The concentration of HS- β -CD was varied from 0.2% to 1%. The resolution between each enantiomer was still satisfactorily preserved ($R_s > 1.5$) and more importantly, the current was brought down to 10.5 μ A at 0.2 % HS- β -CD. At 1 % HS- β -CD, the current was ~ 27.7 μ A and the approximate analysis time for all runs was within 10 min.

This time, the addition of methanol to the BGE did not cause a dramatic loss of resolution. The reason for this is not yet clear. At constant HS- β -CD concentration (1%), the methanol content of the BGE was varied from 0% to 20%. The current was reduced from ~ 27.7 μ A to 15.5 μ A with 20% methanol using a 50-cm long capillary.

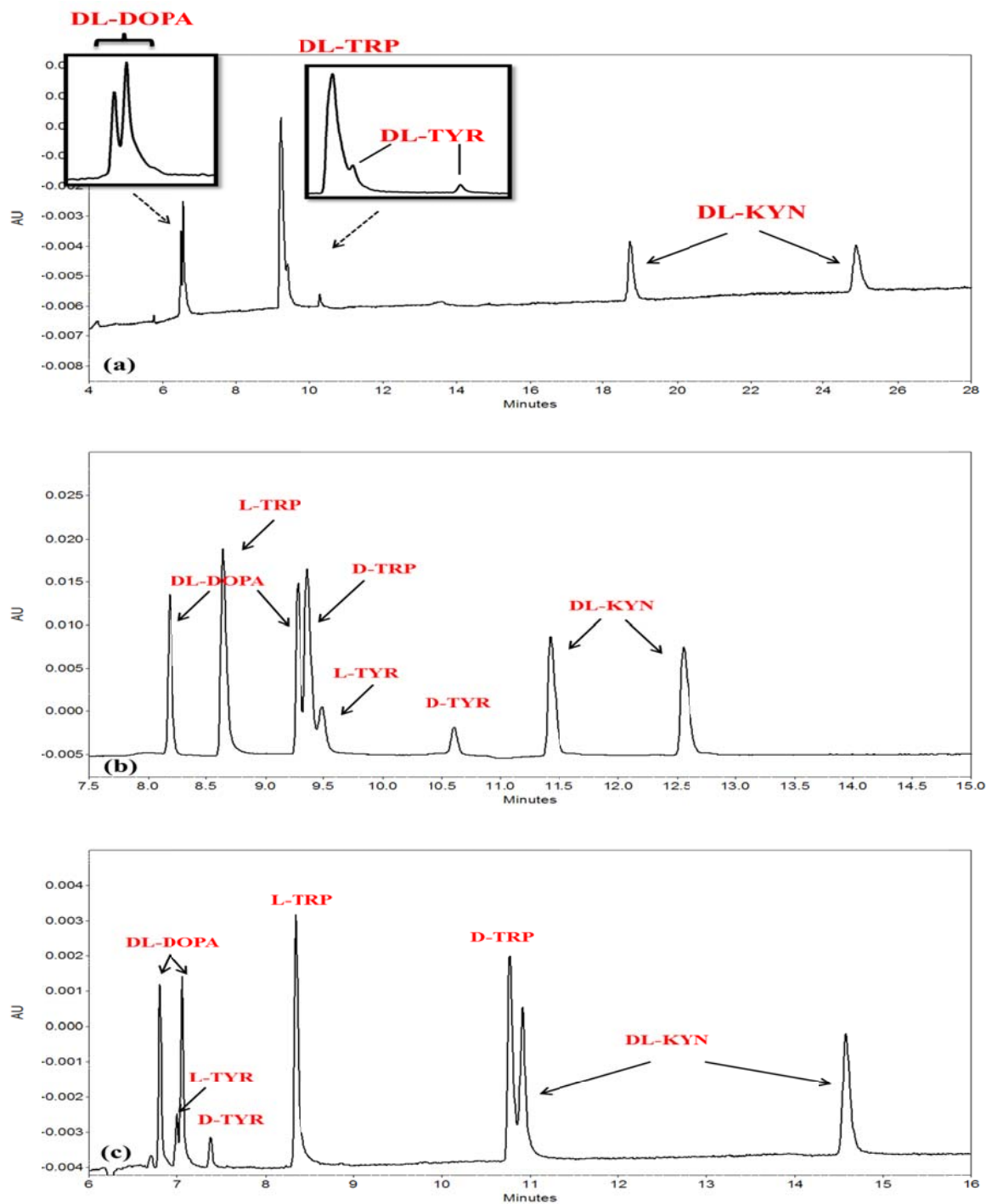


Figure 3.6: Enantiomeric separation of 0.1 mM DL-Trp, DL-Tyr, DL-DOPA, and DL-Kyn on a bare-fused silica capillary: (a) 5 % HS- α -CD CE, (b) 5 % HS- β -CD, and (c) 5 % HS- γ -CD. CE conditions: L_T , 50 cm; BGE, 0.18 % formic acid, (pH 2.5); capillary temperature, 22 °C; wavelength detection, 200 nm; voltage, 15kV.

3.4 CONCLUSIONS

The separation of several racemic amino acids was investigated using native and functionalized CDs. The inclusion selectivity of DL-Trp to α -CD's hydrophobic cavity was found to be dependent on several factors including but not limited to: BGE, electrophoretic mobility of the analyte, EOF, viscosity, and organic modifier. The resolution between D- and L-Trp was found to increase at lower pH values ($\text{pH} < 3$), higher CD concentrations, and longer capillaries. An optimum voltage of 15 kV was obtained which balanced out the band broadening effects caused by joule heating and diffusion.

The second part of this study used a group of charged cyclodextrin derivatives. Excellent enantiomer separations were found for each racemic pair using HS- α -CD, HS- β -CD, and HS- γ -CD. The existence of these derivatized CDs as anions in low pH buffers allowed greater flexibilities in separating cationic analytes. The counter migration phenomenon experienced by the anionic host CDs and cationic analytes is certainly a suitable strategy for CE/MS analysis of chiral compounds. The application of HS-CDs in chiral CE/MS is highly promising.

Chapter 4: Work in progress and future directions

4.1 CHIRAL SEPARATION WITH CE-ESI-MS

The problem of directly spraying non-volatile cyclodextrins into the MS is still the principal challenge for CE-ESI-MS analysis. With the combination of organic modifiers and the use of longer capillaries, we successfully reduced current to within working ESI conditions ($< 15 \mu\text{A}$) in our work. We also started some chiral separations of simple amino acids using our group's home-made CE/MS interface. However, it was the author's decision not to present unfinished work and incomplete data in this thesis. Several strategies such as partial filling and counter migration methods are being studied to prevent the non-volatile CDs from going to the MS analyzer. With the enantioselective power of highly-sulfated cyclodextrins, we can perhaps utilize very low concentrations ($< 0.1\%$) of HS-CDs in the buffer and bypass partial filling techniques without detrimental consequences to the mass analyzer.

4.2 PROSTATE CANCER BIOMARKERS: CLINICAL STUDY PROPOSAL

Our efforts in conducting a biomarker study for prostate cancer research is only one amongst many. Indeed, many of the largest research institutions in the world are currently working in this field. During the last decade, several discoveries for prospective biomarkers have been presented in the scientific community, but only a handful has reached clinical trials stage⁸³.

The suggested guidelines⁸⁴ for developing a successful biomarker qualification study are: (1) development of potential biomarker assay; (2) validation and qualification of biomarker assay; (3) selection of appropriate sample type and collection strategies; (4)

establish relevant control group; and (5) conduct clinical studies to generate data supporting the degree of biomarker “fit of purpose” and clinical qualification. We believe that one of the main problems encountered in this area is a simple oversight on *good laboratory practice* (GLP) and *good clinical practice* (GCP). Although our own biomarker study is still in the early stages, we have taken careful measures in developing and validating our biomarker assay methods. We are currently seeking collaboration with the *Vancouver Prostate Cancer Centre* to obtain urine samples from PCa patients in order to initiate clinical studies. We are discussing important issues such as ethics requirements on research involving human participants; the appropriate number of patients; and a consistent design and efficient protocol for sampling and instrumental analysis. A consultation with biostatisticians might also be an asset for the proper statistical treatment of the acquired data. A small scale clinical trial is currently being conducted to test the feasibility of using the biomarkers discussed in Chapter 2.

Indeed, this project can be an enormous undertaking for our group. It is with great anticipation and hope that this work will be the centrepiece of a much larger clinical trial. I have come to realize that the development of powerful technologies and methodologies brings not only valuable knowledge, but also a sense of responsibility for our society. For many people, the cure for cancer is still a far-fetched dream; however, I believe that a collective effort in cancer research brings us much closer to this goal.

BIBLIOGRAPHY

- (1) Southern, E. M. *J. Mol. Biol.* **1975**, 98, 503-517.
- (2) Consden, R.; Gordon, A. H.; Martin, A. J. P. *Biochem. J.* **1946**, 40, 33-41.
- (3) Wehr, T., Rodríguez-Díaz, R. and Zhu, M. *Capillary Electrophoresis of Proteins*, ed.; Marcel Dekker, Inc.:New York; 1999.
- (4) Swerdlow, H.; Gesteland, R. *Nucleic Acids Res.* **1990**, 18, 1415-1419.
- (5) Zagursky, R. J.; McCormick, R. M. *BioTechniques.* **1990**, 9, 74-79.
- (6) Thundat, T. *Nat. Nanotechnol.* **2010**, 5, 246-247.
- (7) Rech, I.; Marangoni, S.; Gulinatti, A.; Ghioni, M.; Cova, S. *Sens.Actuator B-Chem.* **2010**, 143, 583-589.
- (8) Anderson, N. L.; Anderson, N. G. *Electrophoresis.* **1998**, 19, 1853-1861.
- (9) Fiehn, O. *Plant Mol.Biol.* **2002**, 48, 155-171.
- (10) Woolley, A. T.; Mathies, R. A. *Anal. Chem.* **1995**, 67, 3676-3680.
- (11) Andersen, J. S.; Wilkinson, C. J.; Mayor, T.; Mortensen, P.; Nigg, E. A.; Mann, M. *Nature.* **2003**, 426, 570-574.
- (12) Williamson, A. J. K.; Whetton, A. D. *J. Cell. Physiol.* **2011**, 226, 2478-2483.
- (13) Kaddurah-Daouk, R.; Kristal, B. S.; Weinshilboum, R. M. *Annu. Rev. Pharmacol. Toxicol.* **2008**, 48, 653-683.
- (14) Hjertén, S. *J. Chromatogr.* **1985**, 347, 191-198.
- (15) Horvath, J.; Dolnik, V. *Electrophoresis.* **2001**, 22, 644-655.
- (16) Frazier, R. A., Ames, J. M. and Nursten, H. E. *Capillary Electrophoresis of Food Analysis: Method Development*, 1st ed.; Royal Society of Chemistry:Cambridge, UK; 2000.
- (17) Drozd, J. *J. Chromatogr.* **1975**, 113, 303-356.
- (18) Guzman, N. A.; Majors, R. E. *LC·GC Europe.* **2001**, , 1-9.
- (19) Giddings, J. C. *Unified Separation Science*, 1st ed.; John Wiley & Sons, Inc.:New York; 1991.

- (20) Maxwell, E. J.; Chen, D. D. Y. *Anal. Chim. Acta.* **2008**, 627, 25-33.
- (21) Gross, J. H. *Mass Spectrometry: A Textbook*, 1st ed.; Springer-Verlag:Germany; 2004.
- (22) Watson, J. T. and Sparkman, O. D. *Introduction to Mass Spectrometry: Instrumentation, Application and Strategies for Data Interpretation*, 4th ed.; John Wiley & Sons:England; 2007.
- (23) Boyd, R. K., Basic, C. and Bethem, R. A. *Trace Quantitative Analysis by Mass Spectrometry*, 1st ed.; John Wiley & Sons:England; 2008.
- (24) Helmja, K.; Borissova, M.; Knjazeva, T.; Jaanus, M.; Muinasmaa, U.; Kaljurand, M.; Vaher, M. *J. Chromatogr. A.* **2009**, 1216, 3666-3673.
- (25) Monnig, C. *ABRF Symposium at the 1996 Protein Society Meeting.* **1996**,
- (26) Pantuckova, P.; Gebauer, P.; Bocek, P.; Krivankova, L. *Electrophoresis.* **2009**, 30, 203-214.
- (27) Meng, C. K.; Mann, M.; Fenn, J. B. *Z. Phys. D-Atoms Mol. Clusters.* **1988**, 10, 361-368.
- (28) Maxwell, E. J.; Zhong, X.; Zhang, H.; van Zeijl, N.; Chen, D. D. Y. *Electrophoresis.* **2010**, 31, 1130-1137.
- (29) Kuo, K. C.; Cole, T. F.; Gehrke, C. W.; Waalkes, T. P.; Borek, E. *Clin.Chem.* **1978**, 24, 1373-1380.
- (30) Shoemaker, J. D.; Elliott, W. H. *J. Chromatogr.-Biomed. Appl.* **1991**, 562, 125-138.
- (31) van Kuilenburg, A. B. P.; Stroomer, A. E. M.; van Lenthe, H.; Abeling, N. G. G. M.; van Gennip, A. H. *Biochem. J.* **2004**, 379, 119-124.
- (32) Hagenfeldt, L.; Bjerkenstedt, L.; Edman, G.; Sedvall, G.; Wiesel, F. A. *J. Neurochem.* **1984**, 42, 833-837.
- (33) Allen, R. H.; Stabler, S. P.; Lindenbaum, J. *Metab.-Clin. Exp.* **1993**, 42, 1448-1460.
- (34) Sreekumar, A.; Poisson, L. M.; Rajendiran, T. M.; Khan, A. P.; Cao, Q.; Yu, J.; Laxman, B.; Mehra, R.; Lonigro, R. J.; Li, Y.; Nyati, M. K.; Ahsan, A.; Kalyana-Sundaram, S.; Han, B.; Cao, X.; Byun, J.; Omenn, G. S.; Ghosh, D.; Pennathur, S.; Alexander, D. C.; Berger, A.; Shuster, J. R.; Wei, J. T.; Varambally, S.; Beecher, C.; Chinnaiyan, A. M. *Nature.* **2009**, 457, 910-914.

- (35) Meyer, T. E.; Fox, S. D.; Issaq, H. J.; Xu, X.; Chu, L. W.; Veenstra, T. D.; Hsing, A. W. *Anal. Chem.* **2011**, *83*, 5735-5740.
- (36) Bridges, J. W. In *Recent Advances in Chiral Separations* Stevenson, D., I. D. Wilson; Plenum Press: New York, 1991; pp 1-3.
- (37) European Commission Public Health. http://ec.europa.eu/health/index_en.htm. **2012**, (accessed: 06.02.2012), 11.
- (38) Health Canada. <http://www.hc-sc.gc.ca/dhp-mps/prodpharma/applic-demande/guide-ld/chem/stereo-eng.php>. **2000**, (accessed: 06.02.2012)
- (39) U.S. Food and Drug Administration. <http://www.fda.gov/drugs/GuidanceComplianceRegulatoryInformation/Guidances/ucm122883.htm>. **2011**, (accessed: 06.02.2012)
- (40) McBride, W. G. *Lancet*. **1961**, *2*, 1358.
- (41) Howlader, H.; Noone, A. M.; Krapcho, M.; Neyman, N.; Aminou, R.; Waldron, W.; Altekruse, S. F.; Kosary, C. L.; Ruhl, J.; Tatalovich, Z.; Cho, H.; Mariotto, A.; Eisner, M. P.; Lewis, D. R.; Chen, H. S.; Feuer, E. J.; Cronin, K. A. *SEER Cancer Statistics Review*. **2011**, (04.24.2012)
- (42) Prostate Cancer Canada. <http://www.prostatecancer.ca/Prostate-Cancer/Prostate-Cancer/Statistics>. , 2012
- (43) Catalona, W. J.; Smith, D. S.; Ratcliff, T. L.; Dodds, K. M.; Coplen, D. E.; Yuan, J. J.; Petros, J. A.; Andriole, G. L. *N. Engl. J. Med.* **1991**, *324*, 1156-1161.
- (44) Roobol, M. J.; Schroder, F. H.; Crawford, E. D.; Freedland, S. J.; Sartor, A. O.; Fleshner, N.; Andriole, G. L. *J. Urol.* **2009**, *182*, 2112-2120.
- (45) Clarke, R. A.; Schirra, H. J.; Catto, J. W.; Lavin, M. F.; Gardiner, R. A. *Cancers*. **2010**, *2*, 1125-1154.
- (46) Jamaspishvili, T.; Kral, M.; Khomeriki, I.; Student, V.; Kolar, Z.; Bouchal, J. *Prostate Cancer Prostatic Dis.* **2010**, *13*, 12-19.
- (47) Oresic, M.; Vidal-Puig, A.; Hanninen, V. *Expert Rev. Mol. Diagn.* **2006**, *6*, 575-585.
- (48) Gruson, D.; Bodovitz, S. *Biomarkers*. **2010**, *15*, 289-296.
- (49) Jentzmik, F.; Stephan, C.; Miller, K.; Schrader, M.; Erbersdobler, A.; Kristiansen, G.; Lein, M.; Jung, K. *Eur. Urol.* **2010**, *58*, 12-18.

- (50) Struys, E. A.; Heijboer, A. C.; van Moorselaar, J.; Jakobs, C.; Blankenstein, M. A. *Ann. Clin. Biochem.* **2010**, *47*, 282-282.
- (51) Jiang, Y.; Cheng, X.; Wang, C.; Ma, Y. *Anal. Chem.* **2010**, *82*, 9022-9027.
- (52) Jentzmik, F.; Stephan, C.; Lein, M.; Miller, K.; Kamlage, B.; Bethan, B.; Kristiansen, G.; Jung, K. *J. Urol.* **2011**, *185*, 706-711.
- (53) Cao, D.; Ye, D.; Zhang, H.; Zhu, Y.; Wang, Y.; Yao, X. *Prostate.* **2011**, *71*, 700-710.
- (54) Wu, H.; Liu, T.; Ma, C.; Xue, R.; Deng, C.; Zeng, H.; Shen, X. *Anal. Bioanal. Chem.* **2011**, *401*, 635-646.
- (55) Bianchi, F.; Dugheri, S.; Musci, M.; Bonacchi, A.; Salvadori, E.; Arcangeli, G.; Cupelli, V.; Lanciotti, M.; Masieri, L.; Serni, S.; Carini, M.; Careri, M.; Mangia, A. *Anal. Chim. Acta.* **2011**, *707*, 197-203.
- (56) Meyer, T. E.; Fox, S. D.; Issaq, H. J.; Xu, X.; Chu, L. W.; Veenstra, T. D.; Hsing, A. W. *Anal. Chem.* **2011**, *83*, 5735-5740.
- (57) Issaq, H. J.; Veenstra, T. D. *J. Sep. Sci.* **2011**, *34*, 3619-3621.
- (58) Hewavitharana, A. K. *Eur. Urol.* **2010**, *58*, E39-E40.
- (59) Colleselli, D.; Stenzl, A.; Schwentner, C. *Eur. Urol.* **2010**, *58*, E51-E51.
- (60) Ramautar, R.; Mayboroda, O. A.; Derks, R. J. E.; van Nieuwkoop, C.; van Dissel, J. T.; Somsen, G. W.; Deelder, A. M.; de Jong, G. J. *Electrophoresis.* **2008**, *29*, 2714-2722.
- (61) Ramautar, R.; Torano, J. S.; Somsen, G. W.; de Jong, G. J. *Electrophoresis.* **2010**, *31*, 2319-2327.
- (62) Guo, K.; Li, L. *Anal. Chem.* **2009**, *81*, 3919-3932.
- (63) Cavaliere, B.; Macchione, B.; Monteleone, M.; Naccarato, A.; Sindona, G.; Tagarelli, A. *Anal. Bioanal. Chem.* **2011**, *400*, 2903-2912.
- (64) Heymsfield, S. B.; Arteaga, C.; McManus, C.; Smith, J.; Moffitt, S. *Am. J. Clin. Nutr.* **1983**, *37*, 478-494.
- (65) Clarke, J. T. *Clin. Chem.* **1961**, *7*, 371-&.
- (66) Kollipara, S.; Bende, G.; Agarwal, N.; Varshney, B.; Paliwal, J. *Chromatographia.* **2011**, *73*, 201-217.

- (67) Wishart, D. S.; Knox, C.; Guo, A. C.; Eisner, R.; Young, N.; Gautam, B.; Hau, D. D.; Psychogios, N.; Dong, E.; Bouatra, S.; Mandal, R.; Sinelnikov, I.; Xia, J.; Jia, L.; Cruz, J. A.; Lim, E.; Sobsey, C. A.; Shrivastava, S.; Huang, P.; Liu, P.; Fang, L.; Peng, J.; Fradette, R.; Cheng, D.; Tzur, D.; Clements, M.; Lewis, A.; De Souza, A.; Zuniga, A.; Dawe, M.; Xiong, Y.; Clive, D.; Greiner, R.; Nazyrova, A.; Shaykhutdinov, R.; Li, L.; Vogel, H. J.; Forsythe, I. *Nucleic Acids Res.* **2009**, *37*, D603-D610.
- (68) Wishart, D. S.; Tzur, D.; Knox, C.; Eisner, R.; Guo, A. C.; Young, N.; Cheng, D.; Jewell, K.; Arndt, D.; Sawhney, S.; Fung, C.; Nikolai, L.; Lewis, M.; Coutouly, M.; Forsythe, I.; Tang, P.; Shrivastava, S.; Jeroncic, K.; Stothard, P.; Amegbey, G.; Block, D.; Hau, D. D.; Wagner, J.; Miniaci, J.; Clements, M.; Gebremedhin, M.; Guo, N.; Zhang, Y.; Duggan, G. E.; MacInnis, G. D.; Weljie, A. M.; Dowlatabadi, R.; Bamforth, F.; Clive, D.; Greiner, R.; Li, L.; Marrie, T.; Sykes, B. D.; Vogel, H. J.; Querengesser, L. *Nucleic Acids Res.* **2007**, *35*, D521-D526.
- (69) Human Metabolome Database Version 2. www.hmdb.ca. **2009**, (accessed: 04.18.2012)
- (70) Pirkle, W. H.; Pochapsky, T. C. *Chem.Rev.* **1989**, *89*, 347-362.
- (71) Armstrong, D. W.; Ward, T. J.; Armstrong, R. D.; Beesley, T. E. *Science*. **1986**, *232*, 1132-1135.
- (72) Iwata, Y. T.; Garcia, A.; Kanamori, T.; Inoue, H.; Kishi, T.; Lurie, I. S. *Electrophoresis*. **2002**, *23*, 1328-1334.
- (73) Lipka, E.; Vaccher, M.; Vaccher, C.; Bonte, J. *Anal. Lett.* **2010**, *43*, 2356-2371.
- (74) Rudaz, S.; Le Saux, T.; Prat, J.; Gareil, P.; Veuthey, J. L. *Electrophoresis*. **2004**, *25*, 2761-2771.
- (75) Peng, X. J.; Bowser, M. T.; BritzMcKibbin, P.; Bebault, G. M.; Morris, J. R.; Chen, D. D. Y. *Electrophoresis*. **1997**, *18*, 706-716.
- (76) Fanali, S. *J. Chromatogr. A*. **1996**, *735*, 77-121.
- (77) Mikus, P.; Marakova, K. *Electrophoresis*. **2009**, *30*, 2773-2802.
- (78) Herrero, M.; Simo, C.; Garcia-Canas, V.; Fanali, S.; Cifuentes, A. *Electrophoresis*. **2010**, *31*, 2106-2114.
- (79) Simo, C.; Garcia-Canas, V.; Cifuentes, A. *Electrophoresis*. **2010**, *31*, 1442-1456.
- (80) Lipkowitz, K. B.; Raghothama, S.; Yang, J. *J. Am. Chem. Soc.* **1992**, *114*, 1554-1562.

- (81) Dzygiel, P.; Wieczorek, P.; Jonsson, J. A. *J. Chromatogr. A.* **1998**, *793*, 414-418.
- (82) Leiterman, R. V.; Mulski, M. J.; Connors, K. A. *J. Pharm. Sci.* **1995**, *84*, 1272-1275.
- (83) Parekh, D. J.; Ankerst, D. P.; Troyer, D.; Srivastava, S.; Thompson, I. M. *J. Urol.* **2007**, *178*, 2252-2259.
- (84) Dancey, J. E.; Dobbin, K. K.; Groshen, S.; Jessup, J. M.; Hruszkewycz, A. H.; Koehler, M.; Parchment, R.; Ratain, M. J.; Shankar, L. K.; Stadler, W. M.; True, L. D.; Gravell, A.; Grever, M. R. *Clin. Cancer Res.* **2010**, *16*, 1745-1755.